Certification of thesis work

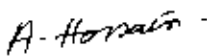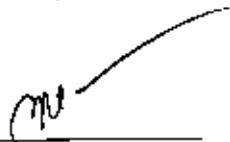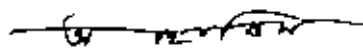The thesis titled "**Investigation of the Magnetoresistive Properties in Double Layered Perovskite Manganites**" submitted by Mohammed Abdul Basith Roll No.040214007 P, Session: April 2002, has been accepted as satisfactory in partial fulfillment of the requirement for the degree of **Master of Philosophy (M.Phil)** in Physics on 11th June, 2005.

BOARD OF EXAMINERS

1. Dr. Mominul Huq   Chairman
   Professor
   Department of Physics. BUET. Dhaka
   (Supervisor)

2. Head   Member
   Department of Physics, BUET. Dhaka

3. Dr. A.K.M. Akther Hossain   Member
   Associate Professor
   Department of Physics, BUET, Dhaka

4. Dr. Md. Abu Hashan Bhuiyan   Member
   Professor
   Department of Physics, BUET, Dhaka

5. Dr A.K.M. Abdul Hakim   Member(External)
   Head, Magnetic Materials Division
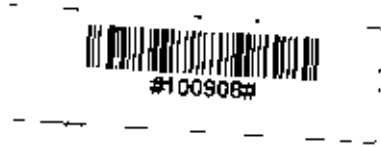   Atomic Energy Centre, Dhaka
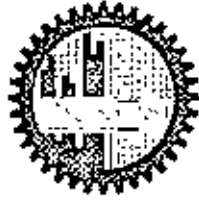
Candidate's Declaration

It is hereby declared that this thesis or any part of it has not been submitted (except publication) elsewhere for the award of any degree or diploma.

Date.
BUET, DHAKA

(Mohammed Abdul Basith)
Roll No. 040214007P
Session . April 2001

i

Abstract

Magnetoresistive properties of $La_{2-2x}Sr_{1+2x}Mn_2O_7$ (x = 0.3-0.5) bulk polycrystalline samples prepared for doping levels x = 0.3 -0.5 and sintered at temperature 1100^0C for 24 hours in air have been investigated from room temperature down to liquid nitrogen temperature using standard four-probe technique. The temperature dependence of normalized resistivity for various polycrystalline samples in zero magnetic field and in a magnetic field of 0.86 Tesla were investigated. The corresponding behavior was observed upon the partial substitution of small amount of Gd in place of La and then also in place of Sr of $La_{2-2x}Sr_{1+2x}Mn_2O_7$ (x = 0.3-0.5) bulk samples. Most of the samples show a metal-insulator (M-I) transition with a peak in the electrical resistivity, ρ_P, at a temperature T_p. This sort of M-I transition may be explained within the framework of interaction mechanisms (double exchange interactions) between the manganese ions that occur via oxygen ions. From the present investigation it is observed that the substitution of a small amount of Gd in place of La remaining the Sr unchanged results in lowering of metal insulator transition temperature by a few Kelvin. As the atomic size of Gd is less than that of La, the substituted Gd ions lower the Mn-Mn exchange interaction substantially by bending the Mn-O-Mn bond angle. The higher percentage of Sr in these compounds enhances paramagnetic insulating phase. But when non-magnetic Sr is replaced with magnetic Gd atom the transition temperature is found to increase dramatically favoring metallic phase. The magnetic property of Gd is thought to be responsible for higher transition temperature. The M-I transition temperature is also increased in presence of 0.86 T magnetic field and this is may be due to the suppression of the spin fluctuations with the applied field in the paramagnetic region. Magnetoresistance measurements were carried out for these polycrystalline bulk samples in a magnetic field of around 0.86 T. Room temperature MR is found to be very low, almost 1.5% ~ 2% and is almost linear with field. The exhibited large MR effects in these compounds at low temperature (78K) and very low field may be associated with magnetic-domain based scattering or spin-polarized tunneling between misaligned grains. In $\rho(T)/\rho(RT) \sim T^{-1}$ plots for the present investigated samples suggest that conduction occurred through a thermally activated process.

Acknowledgements

(Mohammed Abdul Basith)

CONTENTS

✳ List of Figures ✳

List of Tables

List of Symbols, Abbreviations and Nomenclature

T_c	-Curie-Wiess transition temperature
T_p	-Phase transition temperature
T_N	-Neel Temperature
K	-Kelvin
^0C	-Degree centigrade
K_B	-Boltzmann constant $\cong 1.381 \times 10^{-23}$ J/K
eV	-Electron volt $\cong 1.609 \times 10^{-19}$ J
e_g	- Two –fold degenerate state (doublet state)
t_{2g}	-Three-fold degenerate state (triplet state)
DE	-Double exchange
FM	-Ferromagnetic metal
PM	-Paramagnetic metal
CI	-Canted insulator
PI	-Paramagnetic insulator
FI	-Ferromagnetic insulator
MR	-Magnetoresistance
CMR	-Colossal magnetoresistance
GMR	-Giant magnetoresistance
XRD	-X-ray diffraction

CHAPTER 1

Introduction and Motivation
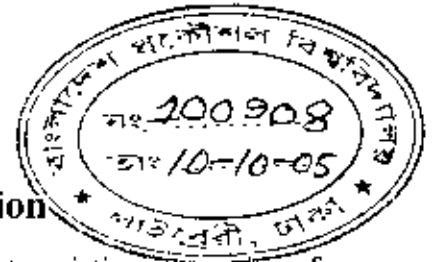
This thesis presents results of an experimental study on magnetoresistive properties of a series of strontium-doped lanthanum manganese oxides. These oxides belong to the broad family of materials known as the mixed-valence manganites, $R_{2-2x}A_{1+2x}Mn_2O_7$ where R is a rare-earth cation such as La, Pr, Y, Nd, etc., and A is an alkaline earth cation such as Ca^{2+}, Sr^{2+}, Ba^{2+}, Na^{2+}, K^{2+}, etc. The designation mixed-valence manganites arises from the fact that the materials may contain manganese in several valence states, depending on the substitution parameter x. The materials are also called perovskite manganites because their crystal structure resembles that of the mineral perovskite, and sometimes doped manganites because the substitution of the R cation with an A cation may serve as hole doping. One of the main features of these materials is the close relationship between magnetism and electrical transport properties.

The mixed-valence manganites have been studied for more than five decades but are still considered modern materials because of their wide potential for technological application. Ferromagnetic manganites may exhibit a magnetoresistance effect, which is comparable to, or even larger than, the giant magnetoresistance (GMR) well known from magnetic multilayers, for which reason it has been designated colossal magnetoresistance (CMR). Magnetoresistance, MR, usually is defined as the relative change of resistance (resistivity) upon a change of the external magnetic field:

$$\frac{\Delta\rho}{\rho_o} = \frac{\rho(H) - \rho(0)}{\rho_0}$$

where $\rho(H)$ and $\rho(0)$ are the resistivities at magnetic field H and zero field, respectively.

The CMR effect is usually obtained at low temperature (below room temperature) and in a high magnetic field (several Teslas), but the practical application demands the operating conditions both at room temperature and a low magnetic field. Potential applications of the CMR effect in mixed-valence manganites include magnetic sensors, magnetoresistive read heads, and magnetoresistive random access memory (MRAM). Colossal

1

Magnetoresistance (CMR) at high temperature and high percentage of spin polarization also makes this class of materials suitable for application in spin electronics or spinotronics.

Among a number of perovskite compounds, hole doped manganese oxide systems have attracted great attention because of their particular magnetotransport phenomena resulting from strong spin-charge coupling [1]. The ABO_3 type compounds with the three-dimensional Mn-O-Mn networks such as $La_{1-x}Sr_xMnO_3$ have long been known to be conducting ferromagnets. The coexistence of metallic conductivity and ferromagnetic coupling in these materials has been explained in terms of double exchange (DE) mechanism [2,3] based on the mixed Mn^{3+}/Mn^{4+} valence states. Doping the insulating $LaMnO_3$ material, in which only Mn^{3+} exists, with the divalent ions (Sr, Ca, Ba etc) causes the conversion of a proportional number of Mn^{3+} to Mn^{4+}. Because of the strong Hund's coupling, the electronic configurations are Mn^{3+} ($t_{2g}^3 e_g^1$) and Mn^{4+} ($t_{2g}^3 e_g^0$). The presence of Mn^{4+}, due to the doping, enables the e_g electron of a Mn^{3+} ion to hop to the neighboring Mn^{4+} ion via DE, which mediates ferromagnetism and conduction. [4].

Most of the attention to date has been focused on doping the parent compound of $LaMnO_3$ with divalent alkaline earths, such as the prototype materials of $La_{1-x}Ca_xMnO_3$. Recently, layered manganites such as the bilayered compound $La_{2-2x}Sr_{1+2x}Mn_2O_7$ have attracted particular attention, since they show an extremely rich variety of magnetic structures as a function of doping and since they allow for the study of dimensionality effects on the electronic and magnetic properties in the doped CMR manganites [5-10]. In general, the compound $La_{2-2x}Sr_{1+2x}Mn_2O_7$ can be viewed as the $n = 2$ member of the Ruddlesden – Popper series $(La_{1-x}Sr_x)_{n+1}Mn_nO_{3n+1}$. The $n = 1$ compound is similar to the La_2CuO_4 structure, and the $n = 2$ compound is analogous to the $Sr_3Ti_2O_7$ structure [11]. The $n = 1$ series of compounds $(R_{1-x}D_x)MnO_4$ exhibit insulating behavior for all x, and in the region $x \cong 0.5$, a charge ordering state appears around $T = 250$ K [12-14]. Previous experiments showed that [4] very strong lattice effects have been realized when the La ions are partially replaced by trivalent and divalent ions of the different size. That is any deviation from the

2

ideal cubic perovskite structure can lead to either a reduction in the Mn-O-Mn bond angle from 180^0, or in the bond length, both directly affecting the double exchange (DE). Most CMR studies were carried out either by doping of the La sites by divalent ions or trivalent atoms of lanthanide series. In the present investigation, trivalent Gd atoms have been doped in both the trivalent La and divalent Sr sites of polycrystalline $La_{2-2x}Sr_{1+2x}Mn_2O_7$ samples. The addition of a small amount of trivalent Gd cation reducing the La will reduce the size of the lanthanide ion across the series, as the ionic sizes of La (atomic radius 1.22 A^0) is greater than that of Gd (atomic radius 1.06 A^0). Consequently, this substitution will modify the electrical properties by lowering the Mn-O-Mn bond angle from 180^0 and thus reducing the electron hopping between Mn^{3+} and Mn^{4+} ions. As the magnetic properties of these samples also depend on the lanthanide ion, the resistivity, phase transition temperature and magnetization properties are expected to change with Gd substitution. It is a special interest of the present investigation is to study the effect of substitution of nonmagnetic Sr^{2+} ion by magnetic trivalent cation Gd, keeping the La site unchanged. Finally, the present investigation aims to study the change in magnetoresistance and ''magnetic phase transition temperature of various polycrystalline samples of Ruddlesden –Popper series $(La_{1-x}Sr_x)_{n+1}Mn_nO_{3n+1}$ with n =2 and thereby to contribute to the elucidation of the physical properties of these fascinating materials.

Jonker and van Santen (1950) reported on the preparation of polycrystalline mixed-valence manganites. They discussed the structural and magnetic properties of $La_{1-x}A_xMnO_3$. They found that the manganites crystallize in the perovskite structure and observed a close relationship between the doping factor x and the structural and magnetic properties. They showed that the end-members with x = 0 and x = 1 are anti-ferromagnetic, while compositions with x = 0.3 are ferromagnetic. Zener [2,3] suggested an explanation for this phenomenon, introducing the so-called double exchange mechanism – a ferromagnetic exchange coupling between magnetic ions in different valence states. Volger [15] measured the magnetoresistance, i.e. the change of resistance due to application of a magnetic field, of a sintered ceramic $La_{0.8}Sr_{0.2}MnO_3$. He observed a negative magnetoresistance of about 8 % near the Curie temperature of the compound. In the

ninetics, new interest in mixed-valence manganites was prompted by the discovery of very large magnetoresistance values in high-quality thin films. Jin et al. [16] reported huge change in resistivity and a corresponding magnetoresistance of 99 % in a La-Ca-Mn-O thin film (at 77 K and with an external field of 6 T). They called this effect colossal magnetoresistance. CMR effect has also been observed for Sr- and Ba-doped lanthanum manganites by von Helmolt et al. in 1994 [17].

The thesis is structured as follows: **Chapter 2** gives a brief overview of the materials as well as different theoretical models such as double exchange model, Jahn-Teller distortion etc. **Chapter 3** deals with the details of sample preparation and characterization experimental techniques used in this thesis. **Chapter 4** presents results on magnetoresistive properties of polycrystalline samples for various doping levels. **Chapter 5** summarizes the findings of this dissertation.

References

[1]   Asano H., Hayakawa J. and Matsui M., (1996), "Giant magnetoresistance of a two-dimensional ferromagnet $La_{2-2x}Ca_{1+2x}Mn_2O_7$", Appl. Phys. Lett., 68, 3638.

[2]   Zener C., (1951), "Low temperature magnetic properties of the Double Exchange mode", Phys. Rev. 82, 403.

[3]   Zener C., (1951), "Interaction between the d shells in the transition metals", Phys. Rev. 81, 440.

[4]   Ahn K.H., Wu X.W , Liu. K., and Chen C.L., (1996), "Magnetic properties and colossal magnetoresistance of $La(Ca)MnO_3$ materials doped with Fe", Phys. Rev. B, 54 15 299.

[5]   Kimura T., Asamitsu A., Tomioka Y., and Tokura Y., (1997), "Interplane tunneling magnetoresistance in a layered manganites crystal", Phys. Rev. Lett. 79, 3720.

[6]   Fukumara T., Sugawara H., Hasegawa T., Tanaka K.,. Sakaki H., Kimura T., and Tokura Y., (1999), "Spontaneous Bubble Domain Formation in a Layered Ferromagnetic Crystal", Science 284, 1969.

[7]   Li Q., Gray K.E., Mitchell J.F., Berger A., Osgood R., (2000) "Double-exchange selection rule for the c-axis conductivity in layered $La_{2-2x}Sr_{1+2x}Mn_2O_7$ single crystals below T_c", Phys. Rev. B 61, 9542.

[8]   Welp U., Berger A., Vlasko-Vlasov V.K., Li Q., Gray K.E., and Mitchell J.F., (2000), "Magnetic anisotropy and domain structure of the layered manganite $La_{1.36}Sr_{1.64}Mn_2O_7$", Phys. Rev. B 62, 8615

[9]   Li Q., Gray K.E , and. Mitchell J.F., (1999), "Spin-Independent and Spin Dependent Conductance Anisotropy in Layered, Colossal-Magnetoresistive Manganite Single Crystals", Phys. Rev. B 59, 9357.

[10]   Welp U., Berger A., Miller D.J., Vlasko-Vlasov V.K., Gray K.E., and. Mitchell J.F, (2000). "Magneto-Optical Imaging of the First Order Spin-Flop Transition in the Layered Manganite $La_{1.4}Sr_{1.6}Mn_2O_7$", J. Appl. Phys. 87, 5043.

[11]   Moritomo Y., Asamitsu A., Kuwahara H., and Tokura Y., (1996) "Giant magnetoresistance manganese oxides with a layered perovskites structure", Nature (London) 380, 141.

[12]   Moritomo Y., Tomika Y., Asamitsu A, Tokura Y. and Matsui Y., (1995), "Magnetic and electronic properties in hole-doped manganese oxides with layered structures : $La_{1-x}Sr_{1+x}MnO_4$", Phys. Rev. B 51, 3297.

[13]   Bao W., Chen C.H., Carter S A., and Cheong S W., (1996) "Electronic Phase Separation and Charge Ordering in $(Sr,La)_2MnO_4$", Solid State Commn. 98, 55.

[14]   Sternlieb B J., Hill J P., Wildgruber U C., Luke G M., Nachumi B., Moritomo Y., and Tokura Y., (1996), "Charge and magnetic order in $La_{0.5}Sr_{1.5}MnO_4$", Phys. Rev Lett. 76, 2169.

[15]   Volger J., (1950) "Further experimental investigations on some ferromagnetic oxidic compounds of manganese with perovskite structure", Physica 20, 49.

[16]   Jin S., McCormack M., Tiefel T. H., and Ramesh R., (1994),"Colossal magnetoresistance in La-Ca-Mn-O ferromagnetic thin films", Journal of Applied Physics, 76 (10), 6929.

[17]   von Helmolt R., Wecker J., Haupt L., and. Bärner K., (1994), "Intrinsic giant magnetoresistance of mixed valence La-A-Mn oxide (A=Ca, Sr, Ba)", Journal of Applied Physics, 76 (10), 6925.

CHAPTER 2
LITERATURE REVIEW

2.1. Overview of the materials

(i)   The CMR materials of the form $R_{1-x}A_xMnO_3$ have attracted most of the research efforts. R stands for a rare earth ion such as La, Nd, Pr or Gd and A denotes a divalent ion such as Ca, Sr or Ba. The manganites crystallize in the perovskites structure, figure 2.1(a). Depending on doping, these compounds show a complex magnetic phase diagram [1]. Ferromagnetism is found in the doping range $0.15<x<0.5$ and the highest Curie temperatures are found in the archetypal compound $La_{1-x}Sr_xMnO_3$ at a doping level $x \sim$ 1/3 with Tc of 270 K (Ca substitution), 360 K (Ba). The manganites show a metal-insulator transition accompanying the ferromagnetic transition. Ferromagnetic order in the mixed-valence manganites is induced by the double exchange mechanism proposed by Zener in 1951. Replacing Mn by Co, Ni, Fe, leads to related families of oxides [2]. Especially the cobaltites show an appreciable magnetoresistance [3] for single crystal work.

(ii)   The Ruddlesden-Popper family of compounds $(R,A)_{n+1}Mn_nO_{3n+1}$[4,5] crystallize in a tetragonal structure consisting of vertex sharing MnO_6 octahedra infinitely extending in the ab-plane and having a thickness of n octahedra along the c-axis, figure 2.1(b) Neighboring layers are separated by a rock-salt layer consisting of $(R,A)_2O_2$. The $n = 1$ member $La_{0.5}Sr_{1.5}MnO_4$ shows charge ordering on the Mn sublattice, but a significant magnetoresistance was not observed. A CMR near the Curie temperature of 126 K was found, however, in the $n = 2$ compound
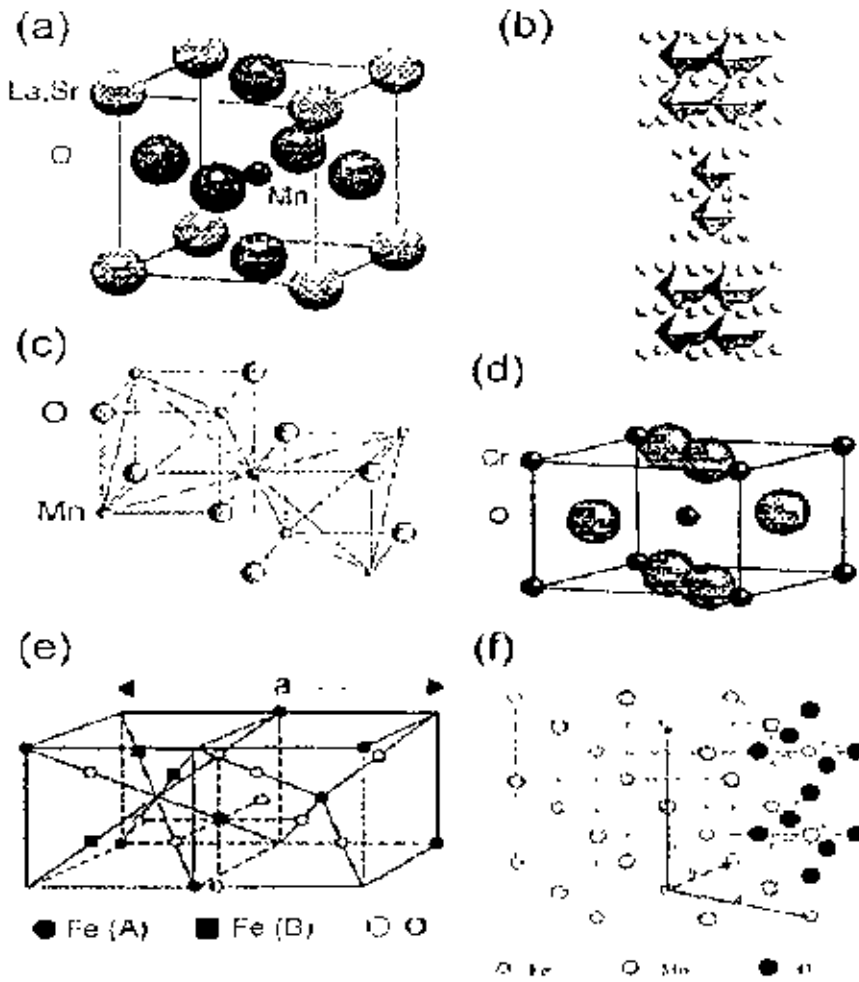
Figure 2.1: Crystal structures of the most important oxides: (a) perovskite stucture ($La_{0.7}Sr_{0.3}MnO_3$); (b) $n = 2$ Ruddlesden–Popper phase ($La_{1.2}Sr_{1.8}Mn_2O_7$, MnO_6 octahedra are shaded, La/Sr ions are drawn as spheres); (c) pyrochlore structure ($Tl_2Mn_2O_7$); (d) rutile structure (CrO_2); (e) inverse spinel structure (Fe_3O_4, for clarity only a quarter of the unit cell is shown) and (f) double-perovskite structure (Sr_2FeMoO_6).

7

$La_{1.2}Sr_{1.8}Mn_2O_7$ [4]. This compound is metallic at low temperatures and semiconducting at higher temperatures similar to the CMR materials. The n = 2 compound $Nd_{1+2x}Sr_{2-2x}Mn_2O_7$ shows a large magnetoresistance, but ferromagnetism was reported to be absent [5]. The Ruddlesden-Popper family of compounds is less investigated.

(iii) $Tl_2Mn_2O_7$ crystallizes in the pyrochlore structure (figure 2.1 (c)); this compound also shows a metal-insulator transition and a large intrinsic magnetoresistance [6,7] near the Curie temperature of about 140 K. In contrast to the manganites, however, the carrier density is low and the ferromagnetism arises from the super-exchange interaction between Mn^{4+} ions. Majumder and Littlewood [8, 9] developed a model for the magnetotransport properties of the pyrochlore based on the assumption of a low-density electron gas coupled to spin fluctuations.

(iv) CrO_2 is a ferromagnet with a Curie temperature of 390 K. It crystallizes in the rutile structure, (figure 2.1 (d)). This oxide is metallic both above and below the Curie temperature.

(v) Magnetite Fe_3O_4, is a ferromagnetic oxide crystallizing in the inverse spinel structure (figure 2.1 (e)) and has the Curie temperature, $T_C = 858$ K. It is therefore often viewed as an ideal candidate for room temperature applications. The temperature dependence of the resistivity is quite complex, changing from semiconductiong to metallic behavior slightly above room temperature and back to semiconducting behavior near to Curie temperature.

(vi) Sr_2FeMoO_6 and Sr_2FeReO_6 are double-perovskite ferromagnets with comparatively high Curie temperatures of about 420 and 400 K, respectively [10-12]. The structure is obtained by doubling the perovskite unit cell, figure 2.1(f). Cation pairs (Fe, Mo), (Fe, Re) order in a rock-salt-like fashion. These compounds were investigated in the 1960s and 1970 [13-16]: interest in these has been revived, since band structure calculations indicated a half metallic-state [10,11]. Often a metallic behavior of the resistivity is observed [12,13,18]; the resistivity, however, depends sensitively on the preparation conditions such as annealing and film growth parameters and semiconducting behavior is sometimes reported [11,17].

8

(vii) $SrRuO_3$ is a metal that undergoes a ferromagnetic transition at 165 K [18-20]. It crystallizes in an orthorhombic structure. $SrRuO_3$ is regarded as a strongly correlated d-band metal [20-23] that falls into the class of 'bad metals' [24]. A 'bad metal' is defined as having an unsaturated resistivity with positive temperature coefficient. The ferromagnetism in $SrRuO_3$ is of itinerant character.

(viii)   There are reports on the resistivity and magnetoresistance of $CaCu_3Mn_4O_{12}$ [25] with Tc of 355 K, $Na_{0.5}Ca_{0.5}Cu_{2.5}Mn_{4.5}O_{12}$ [26] with Tc of 340 K as well as $TbCu_3Mn_4O_{12}$ (Tc = 430 K) and $CaCu_{1.5}Mn_{5.5}O_{12}$ [27]. Whereas Zeng et al [25,26] describe the compounds as ferromagnetic, Troynachuk et al [27] interpret magnetization data as consistent with ferromagnetic order. All compounds show a gradual decrease of the magnetoresistance in large applied fields from some 10 % at low temperature to zero above Tc. These compounds are not important in device fabrication.

(ix)   The chalcogenides $Fe_{1-x}Cu_xCr_2S_4$ shows a moderate magnetoresistance near the Curie temperature [28,29]. Theoretical studies of the electronic structure indicate a half-metallic nature with a gap in the minority density of states [30].

(x)   Stimulated by the intense research on both giant and colossal magnetoresistance, there have been reports on magnetoresistive phenomena in various compounds that do not fall in the classes described above. Here only three reports are mentioned, namely the observation of a large positive magnetoresistance in Ag_2Se and Ag_2Te [31,32] as well as in the ferromagnetic multilayer $LaMn_2Ge_2$ [33].

(xi)   At the end of this list of materials and compounds the case of GdI_2 should be mentioned. GdI_2 shows a ferromagnetic transition close to room temperature; the transition is accompanied by a metal-insulator transition and CMR [34] This observation is especially intriguing, since GdI_2 is nominally isoelectronic to the superconductor $NbSe_2$. In the CMR manganites the situation is similar: substitution of the magnetically active Mn by Cu leads from ferromagnetism in $La_{1-x}Sr_xMnO_3$ to superconductivity in $La_{2-x}Sr_xCuO_4$.

2.2. Classical Double Exchange Model

The transport behavior, especially the simultaneous ferromagnetic and metal-insulator transition, can be understood within the double-exchange model proposed by Zener [35] and further developed by Anderson and Hasegawa [36], de Gennes [37], Searle and Wang [38] and Kubo and Ohata [41].

In the perovskite structure the Mn ions are located on a simple cubic lattice, whereas oxygen ions occupy the centres of the cube edges and the rare earth ion or divalent dopent is located at the cube centre. Thus, the Mn ions are in an octahedral oxygen coordination and, in the ideal structure with tolerance factor (Γ) (described in section 2.3) = 1, the Mn-O-Mn bond angle is 180^0. This leads to a crystal-field splitting of the Mn(3d) orbitals into low-lying t_{2g} and energetically higher e_g levels
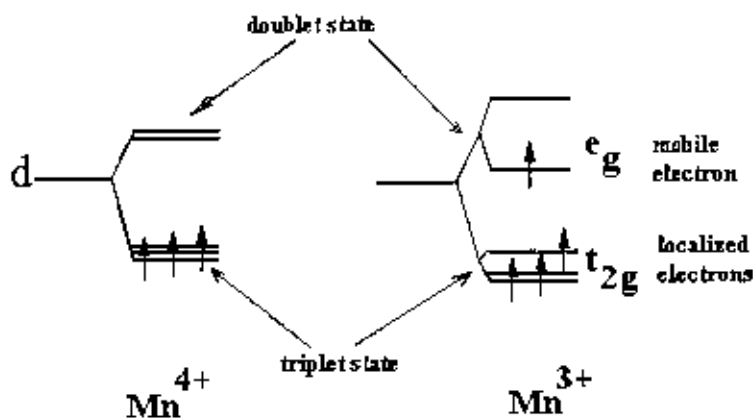
Figure 2.2: Electron states of the outermost 3d energy level of the Mn^{3+} and Mn^{4+} ions.

Within the double-exchange model it is assumed that charge transport occurs on the Mn-O sublattice, whereas the rare earth and alkaline earth ions act only as a charge reservoir. In the parent compound $LaMnO_3$, the manganese ion is a trivalent oxidation state Mn^{3+} with electronic structure $3d^4$. According to Hund's rules three electrons occupy the t_{2g} levels and are coupled into a core spin $S = 3/2$ by the strong intra-atomic Hund's rule coupling. The fourth electron occupies one of the energetically degenerate e_g orbitals. Mn^{3+} is known to be a strong JT (Jahn- Teller) ion and an orthorhombic distortion of the cubic perovskite lattice is indeed found in $LaMnO_3$.

10

On doping with a divalent ion on the rare earth site, i.e. $R_{1-x}A_xMnO_3$, the manganese ions become mixed valent with manganese fractions x in the tetravalent state Mn^{4+} ($3d^3$) and (1-x) in the trivalent state Mn^{3+} ($3d^4$). Zener [35] considered a cluster formed from an oxygen and two Mn ions, one in the trivalent and one in the tetravalent state. The basic idea of double exchange is that the configurations Mn^{3+}-O-Mn^{4+} and Mn^{4+}-O-Mn^{3+} are degenerate leading to a delocalization of the hole on the Mn^{4+} site:

$$t_{2g}^3 e_g^1 - O - t_{2g}^3 e_g^0 \leftrightarrow t_{2g}^3 e_g^0 - O - t_{2g}^3 e_g^1$$
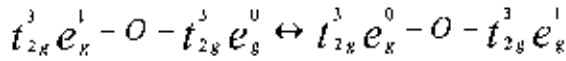
The transfer of a hole occurs simultaneously from Mn^{3+} to O and from O to Mn^{4+}; this process is a real charge transfer process and involves overlap integrals between Mn and O orbitals. Due to the strong Hund's rule coupling energy J_H, Zener [35] suggested that the hole transfer is only possible for parallel orientation of the core spins. This yields the observe simultaneous occurrence of metallic conductivity and ferromagnetism.

Jonker and van Senten [39], and Wollan and Koehler [40], concluded that the exchange coupling in general is

(a) ferromagnetic between Mn^{3+} and Mn^{4+} ions

(b) antiferromagnetic between Mn^{4+} ions

(c) either ferromagnetic or antiferromagnetic between Mn^{3+}

A manganite with an optimal hole concentration or Mn^{4+} content undergoes a paramagnetic insulator (PI) to ferromagnetic metal (FM) like transition as the temperature is decreased, showing a peak in resistivity at a temperature T_{I-M} close to the ferromagnetic Curie temperature Tc. The Tc is related to the strength of the transfer integral between Mn^{3+} and Mn^{4+} ions.

2.3. Jahn-Teller distortion

Most researchers agree that double exchange is the basic mechanism underlying the transport properties of the manganites; it seems, however, not to be sufficient to explain the experimental results. Millis *et al.* [42] were among the first to promote the idea that 'double exchange alone does not explain the resistivity of $La_{1-x}Sr_xMnO_3$' and concluded that lattice distortion plays a necessary and crucial role in the M-I transitions

11

and the resulting CMR effect . Simply lattice distortion occurs due to their different atomic sizes, crystal structure and different magnetic moments.

A simple inspection is enough to discover sources for distortion Firstly, ionic size mismatches: cations A and B can have very different sizes producing tilting and twisting of the oxygen octahedra [43, 44]. This distortion can be estimated by the so-called Goldschmidt tolerance factor

$$\Gamma = \frac{r_{Mn} + r_0}{\sqrt{2}\left(r_{A/B} + r_0\right)}$$

where r stands for the sizes of the different ions in the system. $\Gamma=1$ for a cubic lattice and decrease as the difference in size between A and B increases. It has been found that for oxides and fluorides the perovskite structure types are stable in the range

$$1.0 \geq \Gamma \geq 0.77$$

Tilting of the octohedra can be measured with the distortion of the Mn-O-Mn bond angle $\theta=180^0$ for cubic symmetry. For particular compositions, θ can range from 150^0 to 180^0.

2.4. Resistivity and phase diagram

CMR manganites are oxides of the type $R_{1-x}A_xMnO_3$, where R denotes a rare earth and A is a divalent, often alkaline earth element.
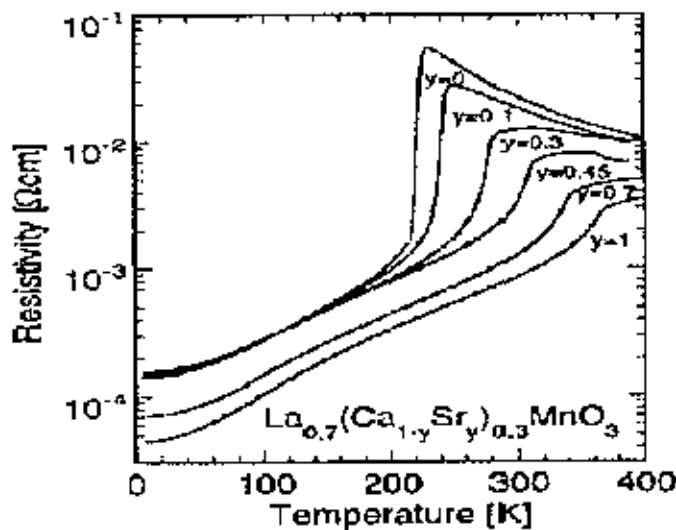
Figure 2.3: Typical resistivity versus temperature curves of La$_{0.7}$(Ca$_{1-y}$Sr$_y$)$_{0.3}$MnO$_3$ single crystals The anomaly at a temperature of 370 K for the $y = 0.45$ doping is due to a structural transition from a low-temperature orthorhombic to a high-temperature rhombohedral phase

12

Typical resistivity versus temperature curves for $La_{0.7}(Ca_{1-y}Sr_y)_{0.3}MnO_3$ single crystals are shown in figure 2.3. At low temperature the resistivity is metallic, rising sharply while going through the ferromagnetic transition and showing semiconducting behavior in the paramagnetic phase in the case of Ca doping, whereas the resistivity in the case of Sr doping remains metallic above the Curie temperature. Accordingly, the ferromagnetic transition in this compound is accompanied by a metal-insulator transition as evidence by the resistivity rise and the negative temperature coefficient of the resistivity in most compounds above Tc.

Much interest has been devoted to the CMR manganites, since these displays a diversified phase diagram.
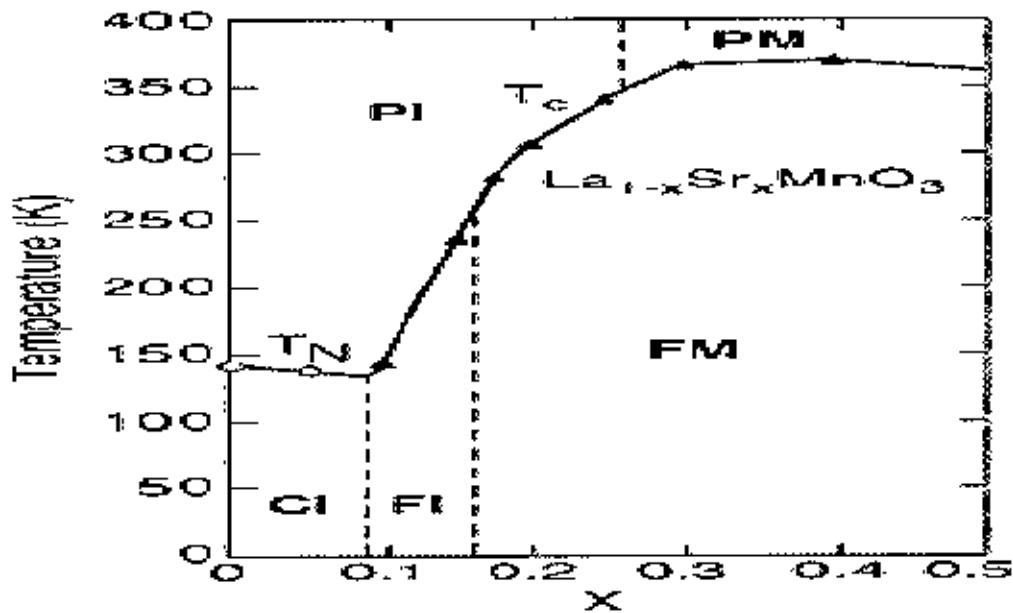
Figure 2.4: Phase diagram of $La_{1-x}Sr_xMnO_3$

2.5. Intrinsic and Extrinsic Magnetoresistance

The aim of this section is to explain the difference between intrinsic and extrinsic magnetoresistance and to illustrate how they can be distinguished from experiment. Some results from the literature are used for exemplification.

Intrinsic Magnetoresistance

Figure 2.5 shows the temperature dependence of the zero field and $\mu_0 H = 5$ T resistivities of a single-crystalline thin film $La_{0.7}Ca_{0.3}MnO_3$ sample (data obtained from Hundley et al. [45]). The corresponding magnetoresistance, MR = ρ_H/ρ_0-1, is shown in the same graph. This sample has no internal grain boundaries so the magnetoresistive response is therefore entirely intrinsic.
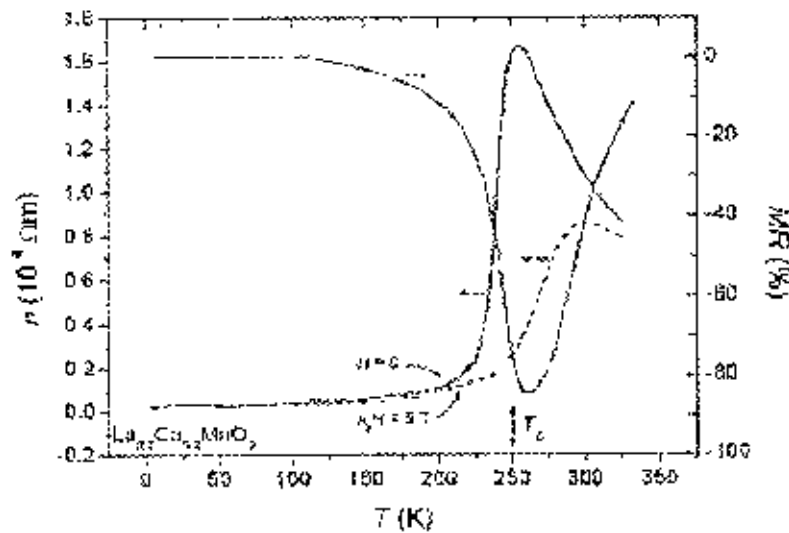
Figure 2.5: Resistivity of single-crystalline thin-film $La_{0.7}Ca_{0.3}MnO_3$ in zero magnetic field and in an applied field of 5 T. The graph shows also the corresponding magnetore-sistance. Adopted from Hundley et al. [45]).

The thin-film substance shows a metal-to-insulator transition coinciding with the ferromagnetic-to-paramagnetic transition at the Curie temperature (250 K). Qualitatively, the temperature dependence of the magnetoresistance can be explained in terms of Zener's double-exchange mechanism. The simplest expression for

14

conductivity is $\sigma = ne\mu$, where n is the number of carriers, e is their charge, and μ their mobility. The metal-to-insulator transition could thus originate from either a change of the number of carriers or a change the mobility of the carriers. In the double-exchange theory the change of hopping mobility is the dominant effect on the conductivity. The transfer integral for electron transport between adjacent Mn sites is $t = t_0 \cos(\theta/2)$ where θ is the angle between the spin directions of the two Mn cores spins. Below the ferromagnetic transition temperature the spin system is ferromagnetically ordered and the probability for electron transfer (and thereby the mobility) is high. The zero-field resistivity shows metallic-like temperature dependence with a positive slope. Around the Curie temperature the spin system becomes disordered because the thermal energy exceeds the ferromagnetic exchange energy. The hopping amplitude decreases and a drastic increase of the zero-field resistivity is observed. Above Tc the resistivity decreases with temperature as expected for an insulator, where transport is thermally activated. The sample exhibits a large negative magnetoresistance peaking just above the Curie temperature. Below T_C the spins align spontaneously and the external field has little influence on θ. The magnetoresistance gradually vanishes when the magnetic moment approaches its saturation value. Near T_C, however, the spin system is highly susceptible to the external field, which causes a substantial change of the local spin disorder and thereby of the carrier mobility. Thus, the field drives the material more metallic. Far above the Curie point the external field can no longer compete with the thermally induced random spin fluctuations and the magnetoresistive response decreases with temperature.

Many research groups have suggested that double exchange alone is not sufficient in order to explain the CMR. The models proposed evoke a competition between double exchange and another mechanism—such as polaron formation due to the strong electron–phonon coupling or localization by spin fluctuations; this competition is supposed to drive the metal–insulator transition. The balance between the two competing mechanisms is very sensitive to an applied magnetic field that suppresses spin fluctuations and enhances the ferromagnetic order. The debate on the essential transport mechanism in the manganites has not yet been decided.

It has been also suggested by Coey *et al.*[46] or von Helmolt *et al.* [47] that the very large change in resistivity observed for manganites is due to magnetic polaron formation in the paramagnetic regime. The e_g electrons may induce a local polarization of its neighboring spins forming a small ferromagnetic entity called a magnetic polaron. According to their suggestion a magnetic polaron can be considered a quasi-particle and it can jump from lattice site to lattice site carrying along its spin polarization. This hopping takes place via thermal activation. Below the Curie temperature (or when a magnetic field is applied) the magnetic polarons are destroyed. This could contribute to the abrupt change of resistivity near T_C. Another kind of polarons, which could be present in manganites, are dielectric polarons formed due to the Coulomb interaction between the electron and its surrounding ionic charges. Dielectric polarons also acts as quasi-particles. The concept of polaron transport in mixed-valence manganites is not yet fully understood.

In theoretical results by Millis et al. [48] the resistivity was obtained from a dynamical mean-field calculation including double exchange and a coupling of carriers to phonons. The calculations show that the resistivity above T_C can be tuned from semiconducting to metallic on decrease of the electron–phonon-coupling strength.

Extrinsic Magnetoresistance

Figure 2.6 (a) compares the temperature dependence of magnetoresistance of a single-crystalline manganite (an epitaxial thin film) with that of a polycrystalline thin film having the same composition ($La_{0.67}Ca_{0.33}MnO_3$). Data was obtained from (Gupta *et al.*, [49]).

Both samples show a magnetoresistance maximum near the Curie temperature, which can be ascribed to intrinsic magnetotransport (the CMR effect). For the epitaxial film the magnetoresistance vanishes at low temperatures, as expected for a single-crystalline material. However, the polycrystalline film shows an increasing magnetoresistance with decreasing temperature.

Figure 2.6 (b) shows the field dependence of magnetoresistance at two different temperatures below the ferromagnetic transition temperature The epitaxial sample

16

shows a linear variation of the magnetoresistance with the applied field. This indicates that the Bloch wall motion and domain rotation in single-crystalline manganites do not dominate transport. The magnetoresistance varies smoothly through the region of domain rotation, which takes place in low fields, so the increasing magnetoresistance is mainly due to enhanced local magnetic order. The magnetoresistance effect is small and decreases with decreasing temperature. The polycrystalline sample exhibits a completely different behavior characterized by two features: 1) a sharp increase of magnetoresistance at low-fields followed by 2) a linear background at higher fields. The slope of the high-field contribution is broadly temperature independent. The low-field magnetoresistance, which is often termed LFMR, increases with decreasing temperature.

It has been suggested by Gupta *et al.*, [49] and Li *et al*, [50] that the low-field magnetoresistance, which is consistently observed in polycrystalline manganites, is due to spin-dependent scattering in grain boundaries. In ferromagnetic metals the exchange energy splits the conduction band into majority and minority carrier bands resulting in a spin imbalance at the Fermi level [51] In mixed-valence manganites the majority and the minority bands are separated by an energy gap arising from the strong intra-atomic coupling between the 3d e_g conduction electrons and the 3d t_{2g} core spins [52]. The spin polarization may therefore approach 100 % at low temperatures (thus, manganites may be characterized as half-metals). In the ferromagnetic state each grain in a polycrystalline manganite may constitute a single magnetic domain [49, 50, 53].

In the virgin state, where no field is applied, the grains have their magnetic moments randomly oriented. The polarized conduction electrons are easily transferred between Mn sites within a magnetic domain. However, an electron traveling across a grain boundary to an adjacent grain (or domain) may become subject to a strong spin-dependent scattering leading to a high zero-field resistivity. A low external field can readily rotate the grain magnetization into a parallel configuration and thereby cause a significant drop in resistivity and low-field magnetoresistance. The degree of spin polarization is temperature dependent and increases with decreasing temperature [54].

17
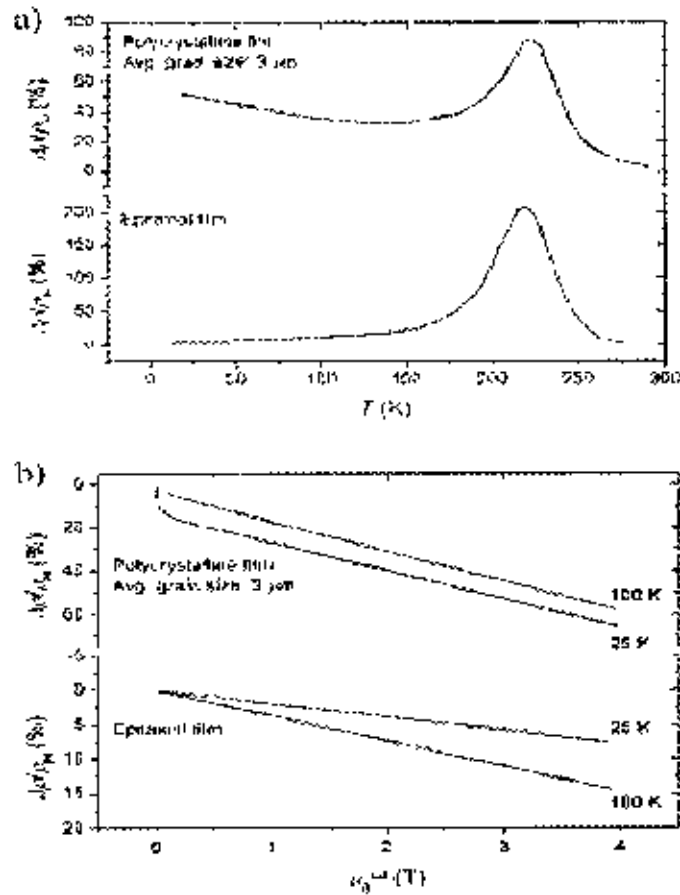
Figure 2.6: Magnetoresistance for a field change of 0 to 2 T versus temperature of poly-crystalline (top panel) and epitaxial (bottom panel) thin film $La_{0.67}Ca_{0.33}MnO_3$. b) Magnetoresistance as a function of applied field taken at 25 and 100 K. Adopted from Gupta *et al.* [49].

This could explain why the low-field magnetoresistance becomes more and more dominant as the temperature is decreased. Spin-dependent scattering of polarized conduction carriers is the dominant mechanism describing spin-valve effects in metallic GMR multilayers [55].

Hwang *et al* [53] offered a different explanation to the low-field magnetoresistance effect observed below the Curie temperature. They compared the magnetoresistive properties of single-crystalline and polycrystalline $La_{0.67}Sr_{0.33}MnO_3$ and also observed LFMR (low field magnetoresistance) in the polycrystalline samples, which was absent in the single crystal. They suggested that the effect was due to spin-dependent tunneling between adjacent grains separated by an insulating grain boundary constituting a tunnel

18

barrier for the spin-polarized conduction electrons. Also within this model the low-field magnetoresistance can be explained by the alignment of magnetizations of neighboring grains.

Spin-dependent scattering or spin-dependent tunneling can explain the low-field magnetoresistance but fail to explain the linear high-field magnetoresistance. Evetts *et al.* [56] suggested that the high-field magnetoresistance is associated with a magnetically mesoscopic disordered interface layer present in the vicinity of grain boundaries (Figure 2.7). The transport mechanism in the interface layer is the same as in the bulk parts of the grains, but the layer has depressed Curie temperature and magnetization, which could be caused by strain, defects and weakened or absent bonds near the grain surface. The high-field MR could be related to alignment of spins in the disordered inter-face layer.
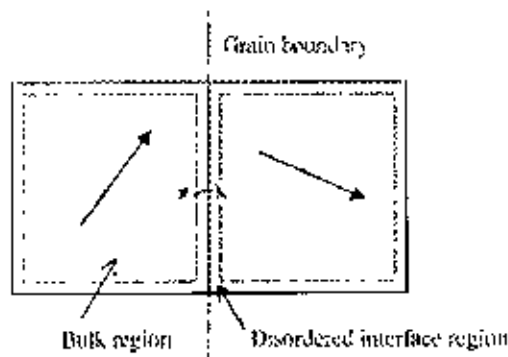
Figure 2.7: Schematic illustration of grain-boundary transport in a polycrystalline mixed-valence manganite. Each grain constitutes a single-magnetic domain. The conduction electrons show a high degree of spin polarization inside the grains. When traveling across the grain boundary conduction electrons may be subject to a strong spin-dependent scattering, which can be reduced if a low external magnetic field aligns the magnetizations of the two grains. Spin alignment in the disordered surface layers gives raise to high-field magnetoresistance.

2.6. Transport properties of few other polycrystalline materials

The effects of grain boundaries on the resistivity and magnetoresistance of polycrystalline manganites compounds were reported very early by Volger et al. [57, 58]. The recent research was initiated by the work of Hwang et al [59] and Gupta et al. [60]. These authors compared the magnetoresistance and magnetization of $La_{0.67}Sr_{0.33}MnO_3$ single crystals and polycrystalline ceramics [59] and $La_{0.67}Ca_{0.33}MnO_3$ and $La_{0.67}Sr_{0.33}MnO_3$ epitaxial and polycrystalline films [60], respectively. Both investigations found that the resistivity and magnetoresisatnce depended sensitively on the microstructure, whereas the magnetization was hardly affected it.
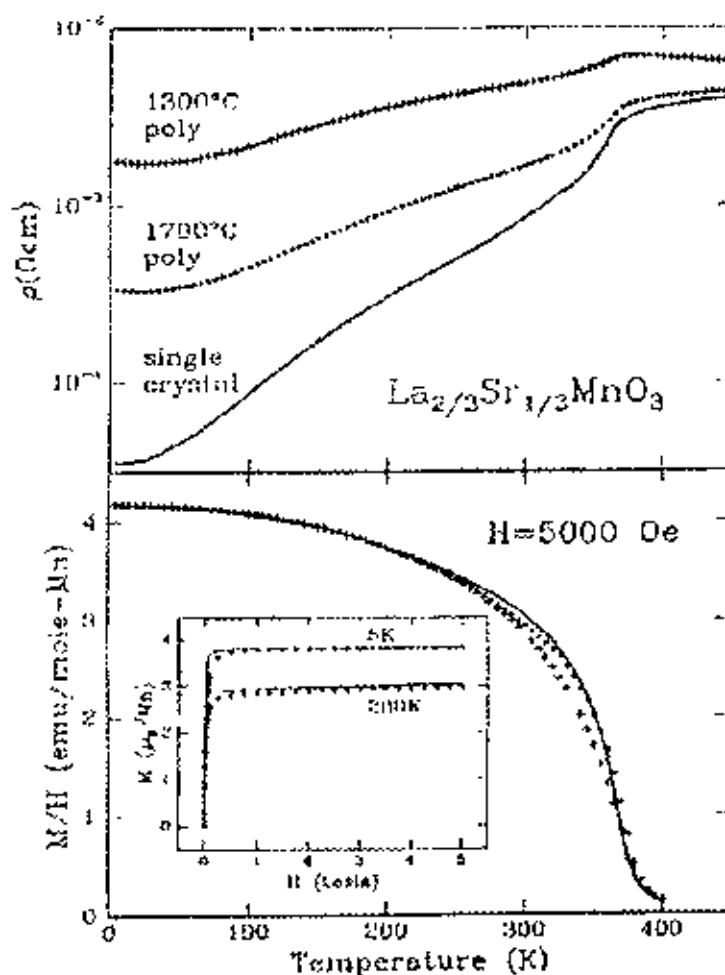
Figure 2.8: Top panel: zero-field resistivity of $La_{0.67}Sr_{0.33}MnO_3$ single crystal and polycrystals as a function of temperature. Bottom panel: magnetization of the samples as a function of temperature measured at $B = 0.5$ T The inset shows the field-dependent magnetization at 5 and 280 K (reproduced from Hwang et al. [59]).
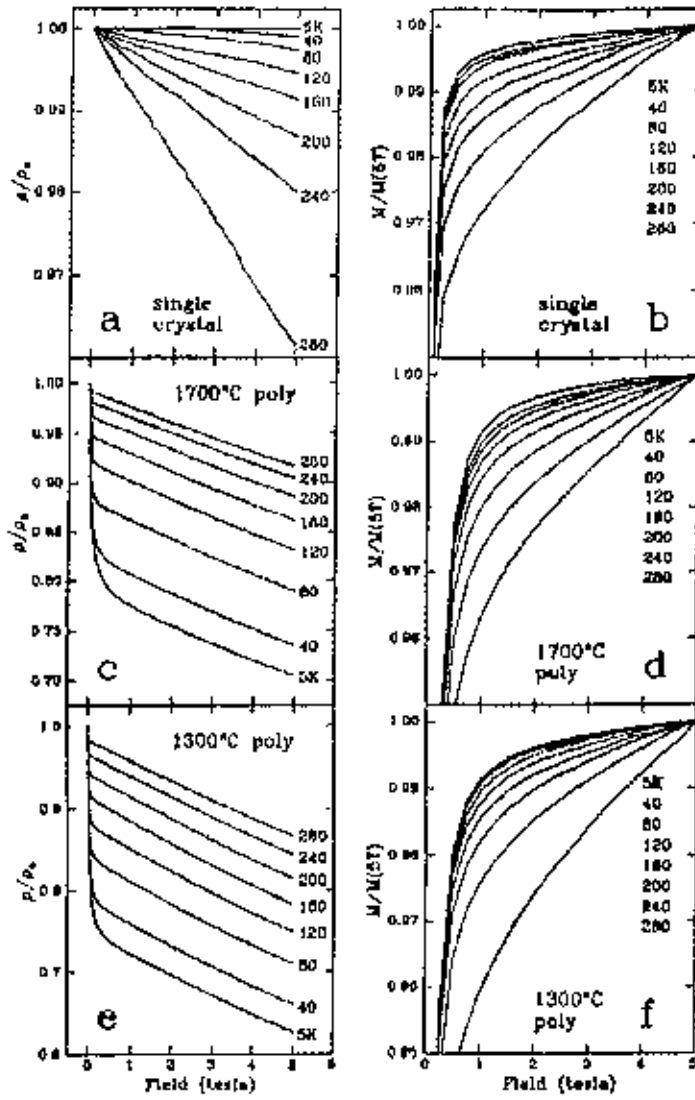
Figure 2.9: Magnetoresistance data of the samples of figure 13. Panels (*a*), (*c*) and (*e*): normalized resistivity ρ / ρ_a as a function of magnetic field ρ_a denotes the zero-field resistivity. Panels (*b*), (*d*) and (*f*): magnetic field dependence of the normalized magnetization (reproduced from Hwang *et al.* [59].

Hwang *et al.* [59] investigated an LSMO single crystal and two LSMO single crystal and two LSMO ceramic samples sintered at 1300 and 1700 ^{0}C, respectively. The sample sintered at the higher temperature had the larger grain size. The data of Hwang *et al.* [59] are reported in figures 2.8. and 2.9.

Figure 2.8 shows the zero-field resistivity and the magnetization of the samples as a function of temperature. Whereas the low-temperature resistivity depends strongly on the microstructure, the magnetization of the three samples is virtually identical. The effect of the grain boundaries on the magnetoresistance is even more dramatic. Figure 2.9 shows the field-dependent resistivity and magnetization of the samples investigated. Whereas the single crystal shows a magnetoresistance linear in magnetic field, the polycrystalline samples show a sharp drop at low magnetic fields followed by a linear dependence at higher fields. Again the field dependence of the magnetization is virtually identical for the three samples. The magnitude of the low-field magnetoresistance increases with decreasing temperature in contrast to the intrinsic magnetoresistance, that has a maximum near the Curie temperature and decreases with decreasing temperature. These results cannot be explained by the intrinsic magnetoresistnce alone, since the intrinsic magnetoresistance is only a function of the magnetization. Hwang *et al.* [59] suggested that the low-field magnetoresistance in polycrystalline samples is due to spin polarized tunneling between misaligned grains

It was shown by Wang *et al.* [61] that, phenomenologically, one has to distinguish weak and strong links between the grains. Only weak links give rise to a considerable low-field magnetoresistance Whereas the microstructural characteristics of the two types of links are not clear, the formation of weak or strong links can be controlled by the fabrication conditions.

References

[1]   Coey J. M. D., (1999), "Powder magnetoresistance", J. Appl. Phys. **85** 5576.

[2]   Goodenough J. B. and Longo M., (1970), Landolt–Bornstein Group III vol 4 126.

[3]   Yamaguchi S., Taniguchi H., Takagi H., Arima T. and Tokura Y., (1995), "Magnetoresistance in metallic crystals of $La_{1-x}Sr_xCoO_3$", J. Phys. Soc. Japan 35 1885.

[4]   Moritomo Y., Asamitsu A., Kuwahara H. and Tokura Y., (1996), "Giant magnetoresistance manganese oxides with a layered perovskites structure", Nature **380** 141

[5]   Battle P. D., Blundellz S. J., Greeny M. A., Hayesz W., Honoldz M.Klehez A. K., Laskeyy N. S, Millburny J. E., Murphyyz L., Rosseinskyy M. J.,Samarinz N. A., Singletonz J., Sluchankoz N. E., Sullivany S. P. and Ventey J. F., (1996), "Colossal magnetoresistance in $Sr_{2-x}Nd_{1+x}Mn_2O_7$ (x = 0.0, 0.1)", J. Phys.: Condens. Matter **8** L427.

[6]   Shimakawa Y., Kubo Y. and Manako T., (1996), "Giant Magnetoresistance in $Tl_2Mn_2O_7$ with the Pyrochlore Structure", Nature 379 53.

[7]   Shimakawa Y., Kubo Y., Hamada N., Jorgensen J.D., Hu Z., Short S., Nohara M and Takagi H., (1999), "Crystal Structure, Magnetic and Transport Properties, and Electronic Band Structure of $A_2Mn_2O_7$ Pyrochlores (A=Y, In, Lu, and Tl)", Phys. Rev. B **59** 1249.

[8]   Majumdar P. and Littlewood P B., (1998), "Magnetoresistance in Mn Pyrochlore: Electrical Transport in a Low Carrier Density Ferromagnet", Phys. Rev. Lett. **81** 1314.

[9]   Majumdar P. and Littlewood P B., (1998), "Magnetoresistance in Mn Pyrochlore: Electrical and doped magnetic semiconductors", Nature **395** 479.

[10]   Kobayashi K-I., Kimura T., Sawada H., Terakura K. and Tokura Y., (1998), "Room temperature magnetoresistance in an oxide material with an ordered double perovskite Sr_2FeMoO_6." Nature **395** 677.

[11]   Kobayashi K-I., Kimura T., Tomioka Y., Sawada H., Terakura K. and Tokura Y., (1999), "Intergrain tunneling magnetoresistance in polycrystals of the ordered double perovskite Sr2FeReO6", Phys. Rev. B **59** 11 159.

[12]   Manako T., Izumi M., Konishi Y., Kobayashi K-I, Kawasaki M. and Tokura Y., (1999), "Epitaxial thin films of ordered double perovskite Sr_2FeMoO_6", Appl. Phys. Lett. 74 2215

[13]   Longo J. M. and Ward R., (1961), "Compounds of Heptavalent Rhenium with the Perovskite Structure", J. Am. Chem. Soc. **83** 1088.

[14]   Sleight A. W., Longo J. M. and Ward R., (1962), "Compounds of Osmium and Rhenium with the Ordered Perovskite Structure", Inorg. Chem. 1 245.

[15]   Sleight A. W. and Weiher J. F., (1972), J. Phys. Chem Solids 33 679

[16] Abe M., Nakagawa T. and Nomura S., (1973), "Magnetic and Mössbauer Studies of the Ordered Perovskites $Sr_2Fe_{1+x}Re_{1-x}O_6$", J. Phys. Soc. Japan 35 1360.

[17] Asano H. *et a.l* (1999), "Pulsed-laser-deposited epitaxial Sr_2FeMoO_6 thin films: Positive and negative magnetoresistance regimes", Appl. Phys. Lett. 74 3696.

[18] Callaghan A., Moeller C. W. and Ward R., (1966), "Magnetic Interactions in Ternary Ruthenium Oxides", Inorg. Chem 5 1572

[19] Longo J. M., Raccah P. M. and Goodenough J. B., (1968), "Magnetic Properties of $SrRuO_3$ and $CaRuO_3$", J Appl. Phys. 39 1327

[20] Cao G., McCall S., Shepard M., Crow J. E. and Guertin R. P., (1997), "Thermal, magnetic, and transport properties of single-crystal $Sr_{1-x}Ca_xRuO_3$ ($0 \leq x \leq 1.0$)", Phys. Rev B 56 321.

[21] Klein L., Dodge J. S., Ahn C. H , Snyder G. J., Geballe T H., Beasley M.R and Kapitulnik A., (1996), "Anomalous Spin Scattering Effects in the Badly Metallic Itinerant Ferromagnet $SrRuO_3$", Phys. Rev Lett. 77 2774.

[22] Fujioka K , Okamato J., Mizokawa T., Fujimori A., Hase I., Abbate M., Lin H. J., Chen C. T., Takeda Y. and Takano M., (1997), "Electronic structure of $SrRuO3$", Phys. Rev. B 56 6380.

[23] Okamoto J., Mizokawa T., Fujimori A , Hase I., Nohara M , Takagi H., Takeda Y and Takano M., (1999), "Correlation effects in the electronic structure of $SrRuO_3$ ", Phys. Rev. B 60 2281.

[24] Emery V. J. and Kivelson S. A., (1995), "Superconductivity in bad metals", Phys Rev. Lett 74 3253.

[25] Zeng Z , Greenblatt M , Subramanian M. A. and Croft M., (1999), "Large Low-Field Magnetoresistance in Perovskite-type $CaCu_3Mn_4O_{12}$ without Double Exchange", Phys. Rev Lett. 82 3135.

[26] Zeng Z., Greenblatt M. and Croft M., (1998), "Large low-field magnetoresistance in $Na_{0.5}Ca_{0.5}Cu_{2.5}Mn_{4.5}O_{12}$, a perovskitelike oxide with hetero-magnetic-ion coupling", Phys. Rev B 58 R595.

[27] Troyanchuk I. P., Khalyavin D. D., Hervieu M., Maignan A., Michel C. and Petrowski K.,(1998), "Magnetoresistance of $TbCu_3Mn_4O_{12}$ and $Ca(Cu_{1.5}Mn_{1.5})Mn_4O_{12}$ Ferrimagnets with Perovskite Structure", Phys. Status Solidi a 169 R1

[28] Ramirez A. P., (1997), "Colossal magnetoresistance," J Phys.: Condens. Matter 9 8171.

[29] Yang Z., Tan S , Chen Z. and Zhang Y., (2000), "Magnetic polaron conductivity in $FeCr_2S_4$ with the colossal magnetoresistance effect", Phys. Rev. B 62 13 872.

[30] Park, J.-H., Chen, C.T., Cheong, S.-W. et al., (1996), "Electronic aspects of the Ferromagnetic Transition in Managanese Perovskites", Phys. Rev Lett. 76 4215.

[31]   Xu R., Husmann A., Rosenbaum T. F., Saboungi M-L., Enderby E. J and Littlewood P. B., (1997), "Large magnetoresistance in non-magnetic silver chalcogenides", Nature 390 57.

[32]   Chuprakov I. S. and Dahmen K. H., (1998), "Large positive magnetoresistance in thin films of silver telluride", Appl. Phys. Lett. 72 2165.

[33]   Mallik R., Sampathkumaran E V. and Paulose P. L., (1997), "Large positive magnetoresistance at low temperatures in a ferromagnetic natural multilayer, $LaMn_2Ge_2$", Appl Phys Lett. 71 2385.

[34]   Ahn K., Felser C., Seshadri R., Kremer R K and Simon A, (2000), "Superconductivity in Layered Lanthanum Carbide Halides: $La_2C_2(X, X')_2$ (X, X'=Cl, Br, I)", J. Alloys Comp. 303–4 252.

[35]   Zener C., (1951), "Interaction between the s-shells in the transition metals: II. Ferromag-netic compounds of manganese with perovskite structure", Phys. Rev. 82 403.

[36]   Anderson P. W. and Hasegawa H., (1955), "Considerations on double exchange", Phys. Rev. 100 675.

[37]   de Gennes P-G., (1960), "Effects of double exchange in magnetic crystals," Phys. Rev. 118 141

[38]   Searle C W and Wang S. T., (1970), "Studies of the ionic ferromagnet (La, Pb)MnO$_3$, V. Electric transport and ferromagnetic properties", Can. J. Phys. 48 2023.

[39]   Jonker G. H. and Van Santen J H., (1950), "Ferromagnetic compounds of manganese with perovskite structure", Physica 16 337

[40]   Wollan E O and Koehler W.C., (1955), "Neutron diffraction study of the magnetic properties of the series of perovskites- type compounds [(1-x)La,xCa]MnO$_3$", Phys Rev. 100 545.

[41]   Kubo K. and Ohata N. (1972), "A quantum theory of double exchange ", J. Phys. Soc. Japan 33 21.

[42]   Millis A J., Littlewood P. B. and Shraiman B. I. (1995), "Double exchange alone does not explain the resistivity of $La_{1-x}Sr_xMnO_3$",Phys Rev. Lett 74 5144.

[43]   Foncuberta J., Martinez B., Sefar A., Pinol S., Garcia-Munoz J..L. and Obradors X., (1996), "Colossal Magnetoresistance of Ferromagnetic Manganites: Structural Tuning and Mechanisms," Phys. Rev. Lett. 76, 1122.

[44]   Radaelli P.G. Iannone G., Marezio M., Hwang H.Y, Cheong S W, Jorgensen J.D and Argyriou D.N, (1997), "Structural effects on the magnetic and transport properties of perovskite $A_{1-x}A'_xMnO_3$ (x = 0.25, 0.30)," Phys Rev. B 56, 8265.

[45]   Hundley M. F., Hawley M., Heffner R. H., Jia Q. X., Neumeier J. J., and Tesmer J, (1995), "Transport-magnetism correlations in the ferromagnetic oxide $La_{0.7}Ca_{0.3}MnO_3$,",Appl. Phys. Lett , 67 (6), 860.

[46] Coey, J. M. D., Viret M , and von Molnar S , (1999). "Mixed-valence manganites", Advances in Physics, **48** (2). 167.

[47] von Helmolt R , Wecker J., Haupt L, and. Bärner K.,(1994). "Intrinsic giant magnetoresistance of mixed valence La-A-Mn oxide (A = Ca, Sr, Ba)", Journal of Applied Physics, 76 (10), 6925

[48] Millis A. J., Mueller R and Shraiman B. I., (1996), "Fermi-liquid-to-polaron crossover. II. Double exchange and the physics of colossal magnetoresistance", Phys Rev B 54 5405.

[49] Gupta, A., G. Q. Gong, G. Xiao, P R. Duncombe, P. Lecoeur, P. Trouilloud, Y Y Wang. V P. Dravid, and J. Z. Sun (1996), "Grain-boundary effects on the magne-toresistance properties of perovskite manganite films", Phys. Rev. B, **54** (22), R15629.

[50] Li X. W., Gupta A , Xiao G , Gong G. Q.. and Gong G. Q., (1997), "Low-field magne-toresistive properties of polycrystalline and epitaxial perovskite manganite films", Appl Phys Lett., **71** (8), 1124.

[51] Gupta A. and Sun J. Z., (1999), "Spin-polarized transport and magnetoresistance in mag-netic oxides", Journal of Magnetism and Magnetic Materials, **200**, 24.

[52] Okimoto Y., Katsufuji T., Ishikawa T., Urushibara A., Arima T., and. Tokura Y., (1995), "Anomalous variation of optical spectra with spin polarization in double-exchange ferromagnet: $La_{1-x}Sr_xMnO_3$", Phys. Rev. Letters, 75 (1), 109.

[53] Hwang H.Y, Cheong S.-W, Radaelli P G, Marezio M. and Batlogg B , (1995), " Lattice effects on the magnetoresistance in doped $LaMnO_3$," Phys. Rev. Lett. **75**, 914.

[54] Ju S , Sun H., and Li Z., (2002), "Study of magnetotransport in polycrystalline perovskite manganites", Journal of Physics Condensed Matter, **14**, L631.

[55] Tumanski, S., (2001), "Thin film magnetoresistive sensors", Bristol: Institute of Physics Publishing.

[56] Evetts, J E , Blamire M. G., Mathur N. D, Isaac S P , Teo B., Cohen L. F., and.Macmanus-Driscol J. L., (1998), "Defect-induced spin disorder and magnetoresistance in single-crystal and polycrystal rare-earth manganite thin film", Philosophical Transactions of the Royal Society London A, **356**, 1593.

[57] Volger J., (1950) "Further experimental investigations on some ferromagnetic oxidic compounds of manganese with perovskite structure", Physica 20, 49.

[58] van den Brom W. E. and Volger J., (1968). Phys. Lett A **26** 197.

[59] Hwang H. Y., Cheong S-W., Ong N. P. and Batlogg B., (1996), "Spin-Polarized Intergrain Tunneling in $La_{2/3}Sr_{1/3}MnO_3$", Phys. Rev Lett 77 2041.

[60] Gupta A., Gong G. Q , Xiao G , Duncombe P. R., Lecoeur P., Trouilloud P.,Wang Y. , Dravid V P. and Sun J. Z., (1996), "Grain-boundary effects on the magnetoresistance properties of perovskite manganite films." Phys.Rev. B 54 R15 629.

[61] Wang H. S. and Li Q , (1998). "Stain-induced large low-field magnetoresistance in $Pr_{0.67}Sr_{0.33}MnO_x$ ultrathin films", Appl. Phys. Lett 73 2360.

CHAPTER 3

Synthesis and Characterization of the Samples

In this chapter basic techniques of sample preparation and experimental technique are discussed.

3.1. Material Synthesis and sample preparation

Samples for the present investigation were prepared using conventional solid-state reaction method. In solid-state reaction method, appropriate amounts of two or more chemical compounds are carefully ground together and mixed thoroughly in a mortar or pestle or ball mills with acetone for homogenization. Ground powders are then calcined in air or in oxygen at a temperature above 1173 K (900^0 C) for several hours to remove the unwanted oxides present in the chemicals. Then they are reground and reheated. This process is continued until the mixture is converted into the correct crystalline phase. This calcined material are then ground to fine powders and palletized in a hydraulic press. Afterwards, sintering is done at different temperatures (below the melting point of the materials) in air or any controlled atmosphere.

The other methods for sample preparation are solution method, melt-quenched or glas ceramic method, thin film method etc.

3.2. Characterization Techniques

After the preparation of the sample, they need to be characterized in different ways to study their physical properties. It would provide the necessary feedback to improve the method of preparation of the grown material. In the present investigation, Powder X-ray diffarction is employed to characterize homogenity of the crystalline powder.

3.3. Lattice Planes and Bragg's Law

The peaks in an X-ray diffraction pattern are directly related to the atomic distances. Let us consider an incident X-ray beam interacting with the atoms arranged in a periodic manner as shown in figure 3.1. The atoms, represented as black spheres in the

graph, can be viewed as forming different sets of planes in the crystal (lines in graph on (a)).
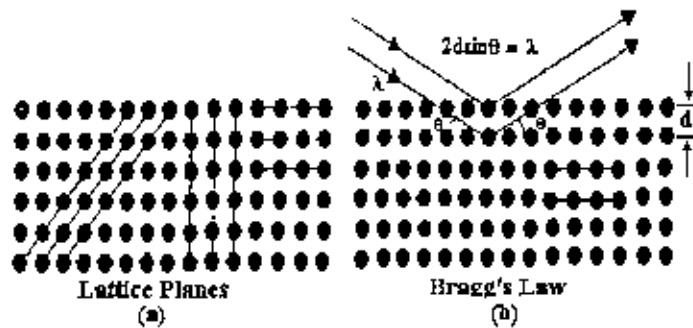
Figure 3.1: Bragg's law of diffraction (a) Different forms of lattice planes, (b) diffraction from atoms

For a given set of lattice plane with an inter-planner distance of d, the condition for a diffraction (peak) to occur can be simply written as

$$2d_{hkl}Sin\theta = n\lambda$$

which is known as the Bragg's law. Here, λ is the wavelength of the X-ray, θ is the scattering angle, and n is an integer representing the order of the diffraction peak.

3.4. The van der Pauw method

The van der Pauw technique [2,3] is based on four point measurements, provided that certain conditions are fulfilled :

- The contacts should be on the circumference of the sample (or very close to the boundary as possible)
- The contacts should be sufficiently small (or as close as possible)
- The sample is to be homogeneous and thin relative to the other dimensions
- The surface of the sample is to be singly connected, i.e. the sample should not have isolated holes

Figure 3.2 shows the four contacts on the circumference of the disc shaped (irregular shaped) sample. For a fixed temperature, we define resistance $R_{AB,CD}$ as the potential difference is V_D-V_C between the contacts D and C per unit current I_{AB} through the

28

contacts A and B . The current enters the sample through the contact A and leaves it through the contact B.

$$R_{AB,CD} = \frac{V_D - V_C}{i_{AB}} \quad (3.1)$$

Analogously we define:

$$R_{BC,DA} = \frac{V_A - V_D}{i_{BC}} \quad (3.2)$$
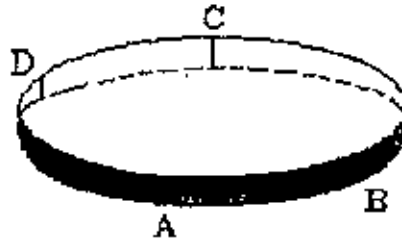
Figure 3.2: The four electrical contacts on the circumference of the disc shaped samples.

Van der Pauw method is based on the theorem that between $R_{AB,CD}$ and $R_{BC,DA}$ there exists the simple relation:

$$\exp\left(-\frac{\pi d}{\rho} R_{AB,CD}\right) + \exp\left(-\frac{\pi d}{\rho} R_{BC,DA}\right) = 1 \quad (3.3)$$

Where d is the thickness of the uniform disc shaped sample and ρ is the resistivity of the material. If d and the resistances $R_{AB,CD}$ and $R_{BC,DA}$ are known, then in Eq. 3.3, ρ is the only unknown quantity.

29
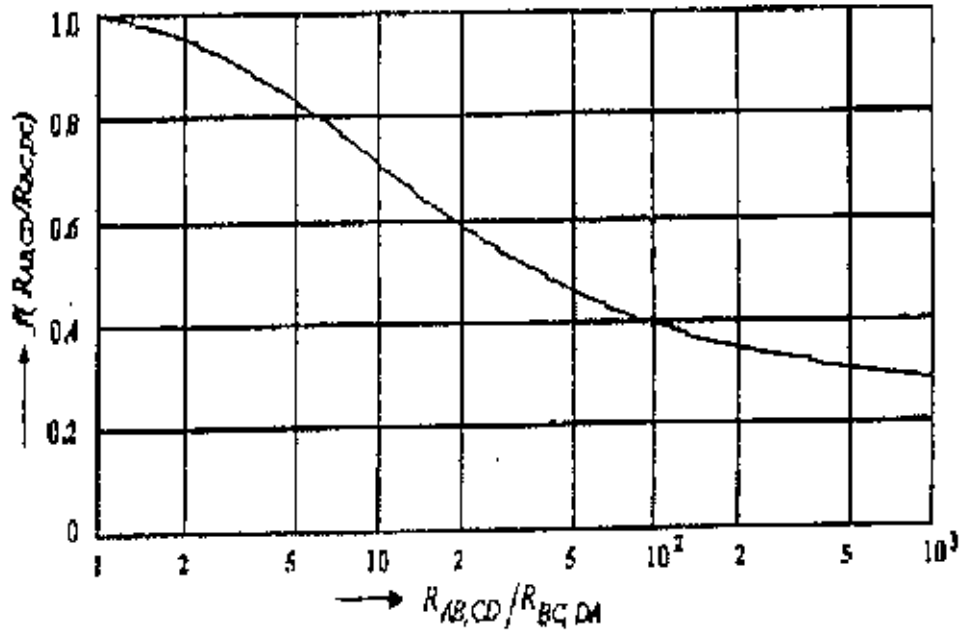
Figure 3.3: The function f(Q) for determining the resistivity of the sample

In the general case, it is not possible to express ρ explicitly in known functions. The solutions can, however, be written in the from

$$\rho(T) = \frac{\pi d}{\ln 2}\left(\frac{R_{AB\,CD} + R_{BC\,DA}}{2}\right)f\left(\frac{R_{AB\,CD}}{R_{BC\,DA}}\right) \qquad (3.4)$$

where f is a factor which is a function only of the ratio $R_{AB\,CD}/R_{BC\,DA}$ and satisfies the relation

$$\cosh\left\{\frac{(R_{AB\,CD}/R_{BC\,DA})-1}{(R_{AB\,CD}/R_{BC\,DA})+1}\times\frac{\ln 2}{f}\right\} = \frac{1}{2}\exp\frac{\ln 2}{f} \qquad (3.5)$$

If we assume $R_{AB\,CD}/R_{BC\,DA}=Q$, then Eq. 3.5 becomes

$$\frac{Q-1}{Q+1} = \frac{f}{\ln 2}\text{arccos}\,h\left\{\frac{\exp(\ln 2/f)}{2}\right\} \qquad (3.6)$$

A plot of the function is shown in figure 3.3.

3.5. Preparation of the Present Samples

Polycrystalline samples were prepared using the conventional solid-state reaction technique. Stoichiometric amounts of raw materials La_2O_3 (99.99%), $SrCO_3$ (99.99%), Gd_2O_3 (99.99%) and $MnCO_3$ (99.99%) were well mixed, then calcined at 1100^0 C in air for 24 hours. The resulting powder samples were then reground and sintered at 1100^0 C for 48-50 hrs in air with one intermediate grinding. Before the final sintering step at 1100^0 C for 24 hrs, the samples were pressed into pellets. The resulting pellets were subjected to electric and magnetic investigation. The specimen's crystallinity & structure were checked by x-ray diffractometry.

3.6. Methodology

The DC electrical resistivity for various polycrystalline samples was measured from room temperature down to liquid nitrogen temperature using standard four-probe method. The temperature dependence of normalized resistivity, $\rho(T)/\rho(RT)$ at zero applied magnetic field for various polycrystalline samples and the corresponding behavior in presence of 0.86 T applied magnetic field have been investigated. Magnetoresistance measurements were carried out in a magnetic field of around 0.86 Tesla in the temperature range 78K to 300K.

3.7. Apparatus used for the present investigation

A liquid nitrogen cryostat was designed previously for the purpose of low temperature magnetotransport measurements. It is made up of nonmagnetic concentric stainless steel tubes. Schematic diagram of the locally fabricated liquid nitrogen cryostat is shown in figure 3.4 and this cryostat was used for the present investigation.

31
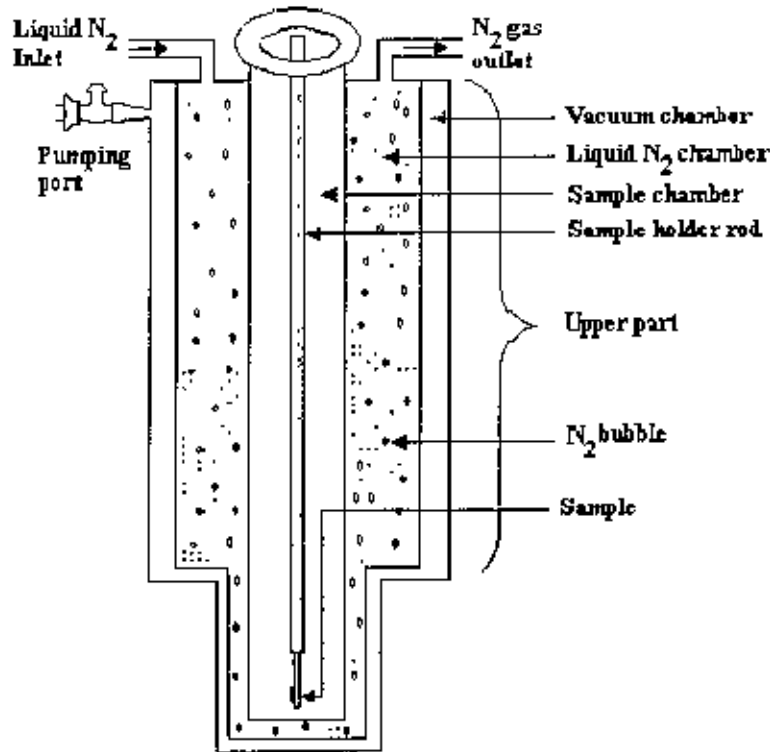
Figure 3.4: Schematic diagram of the liquid nitrogen cryostat

To study magneto-transport properties, an electromagnet was also constructed. In constructing the present electromagnet, commercial mild steel bar for the body of the electromagnet and soft iron cylindrical rod for pole pieces, which were available in the local market was used .
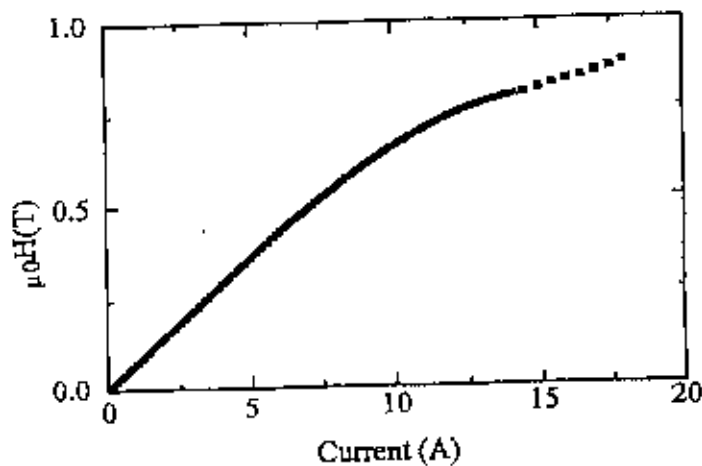
Figure 3.5: Calibration of the locally fabricated electromagnet (gap 3.8 cm)

The electromagnet used for the dc electrical resistivity and magnetoresistance measurement is shown in figure 3.6. Figure 3.8 shows variations of magnetic field as a function of current with constant pole gap 3.8 cm.
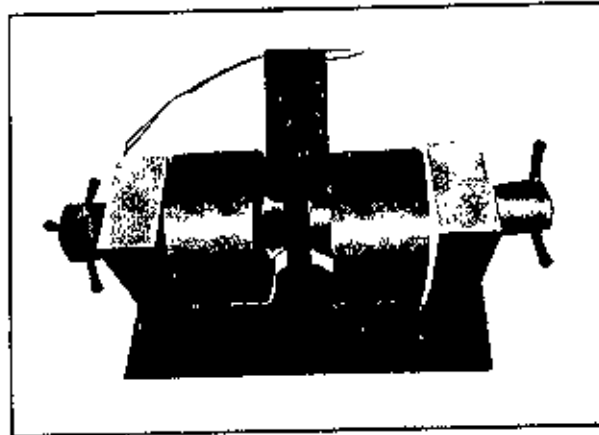
Figure 3.6: Schematic diagram of the electromagnet

A schematic diagram of the sample rod used for the present investigation is shown in figure 3.7.

Multi-pin connectors

Hollow tube

Connecting wire (50 μm silver wir
Sample
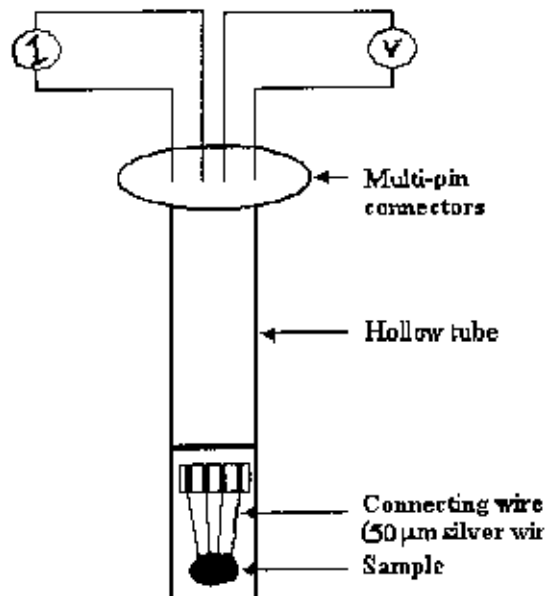
Figure 3.7. Schematic diagram of the sample holder
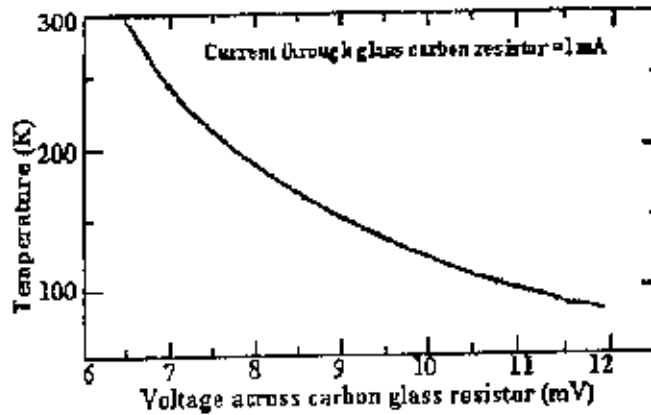
Figure 3.8: Calibration curve of the temperature sensor (Lakeshore Carbon Glass Resistor)

This sample probe is used for four point resistance measurements. At first we thought temperature of the sample would be measured using a thermocouple. However, we have found a problem of using thermocouple for temperature measurements. As we need to airtight the sample space, the temperature probe must be soldered in the two pins in the multi-pin connector. When we will solder a thermocouple with pin a third metal junction appears and as a result it is very difficult to measure temperature accurately. For this reason we have decided to use a carbon glass resistor. For the magnetoresistance measurements, we have to apply magnetic field in the sample space. The carbon glass resistor has a very weak sensitivity to the magnetic field.

References:

[1] Scofield J.H., (1987) "AC method for measuring low frequency resistance fluctuation spectra", Review of Scientific Instruments, **58**, 985.

[2] van der Pauw L.J., (1958) "A method of measuring specific resistivity and Hall effects of discs of arbitrary shape", Philips Research Reports, **13**, 1-9.

[3] van der Pauw L.J., (1958) "A method of measuring specific resistivity and Hall effects of discs of arbitrary shape", Philips Technical Review, **20**, 220-224.

CHAPTER 4

Results and Discussion

The various polycrystalline samples sintered at temperature 1100^0C have been investigated. X-ray diffraction analysis was performed on these samples and XRD patterns were discussed to observe the samples crystallinity and phase purity. The electrical transport and magnetoresistive properties were measured from room temperature down to liquid nitrogen temperature in zero field and in an applied magnetic field of 0.86T. The effect of replacing La in $La_{2-2x}Sr_{1+2x}Mn_2O_7$ (x = 0.3-0.5) by small amount of Gd ions keeping Sr unchanged were investigated in the same temperature region both at zero field and at an applied magnetic field of 0.86 T. The corresponding behavior was also observed by adding magnetic Gd in place of nonmagnetic Sr remaining the amount of La unchanged. Magnetoresistance (MR) measurements were carried out and the MR behavior was discussed as a function of magnetic field both at room temperature and at liquid nitrogen temperature. Activation energies for these polycrystalline samples were calculated to elucidate whether the process is thermally activated or not.

4.1 X-ray diffraction analysis

X-ray diffraction analysis was performed on the investigated polycrystalline samples to examine phase purity and homogeneity. Figure 4.1.1 shows the X-ray diffraction pattern for nine polycrystalline samples and Table 4.1 gives the comparative peak position observed for the same samples X-ray diffraction pattern have confirmed the single phase structure of all the samples with no significant trace of impurity.

Table 4.1: X-ray diffraction peak positions for various polycrystalline samples

| Sample Compositions	X-ray diffraction peak position 2θ (degree)					
	1st	2nd	3rd	4th	5th	6th
$La_{1.4}Sr_{1.6}Mn_2O_7$	14.48	20.80	25.60	29.60	33.40	39.80
$La_{1.2}Sr_{1.8}Mn_2O_7$	14.52	20.80	25.60	29.80	33.40	39.70
$La_{1.0}Sr_{2.0}Mn_2O_7$	14.40	20.70	25.40	29.70	33.20	39.60
$La_{1.2}Gd_{0.2}Sr_{1.6}Mn_2O_7$	14.60	20.80	25.65	29.90	33.50	39.80
$La_{1.0}Gd_{0.2}Sr_{1.8}Mn_2O_7$	14.50	20.75	25.60	29.70	33.60	39.70
$La_{0.8}Gd_{0.2}Sr_{2.0}Mn_2O_7$	14.55	20.95	25.80	30.00	33.60	39.80
$La_{1.0}Gd_{0.4}Sr_{1.6}Mn_2O_7$	14.50	20.75	25.60	29.70	33.60	39.95
$La_{1.0}Gd_{0.6}Sr_{1.4}Mn_2O_7$	14.70	21.00	25.80	29.80	33.55	39.80
$La_{1.0}Gd_{0.8}Sr_{1.2}Mn_2O_7$	14.50	20.80	25.60	29.70	33.60	39.60
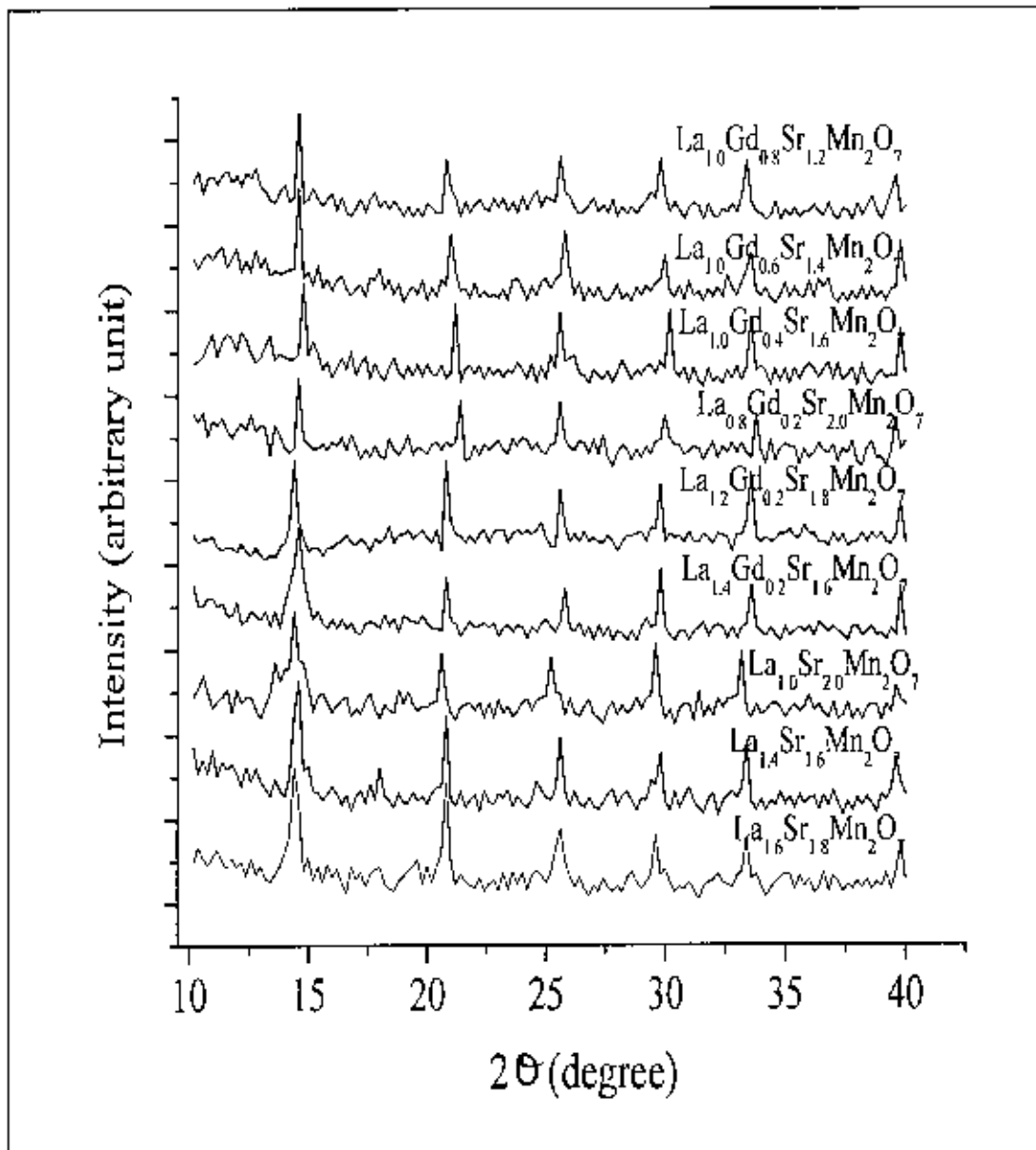
Figure 4.1.1: X-ray diffraction patterns of polycrystalline bulk samples

4.2. DC electrical resistivity

The DC electrical resistance for various $La_{2-2x}Sr_{1+2x}Mn_2O_7$ polycrystalline samples prepared for doping levels x = 0 3-0.5 and sintered at temperature 1100^0C for 24 hours in air have been investigated from room temperature down to liquid nitrogen temperature by using standard four-probe technique.

The temperature dependence of normalized resistivity, $\rho(T)/\ \rho(RT)$, at zero applied magnetic field for various $La_{2-2x}Sr_{1+2x}Mn_2O_7$ (x = 0.3-0.5) bulk samples sintered at 1100^0C are shown in figure 4.1. Figure 4.2 shows the corresponding behavior in presence of 0.86T-applied magnetic field. Polycrystalline samples $La_{1.4}Sr_{1.6}Mn_2O_7$ and $La_{1.2}Sr_{1.8}Mn_2O_7$ show an insulator-metal transition with a peak in the electrical resistivity, ρ, at a temperature Tp (Table 4.2) but such a transition does not occur for sample $La_{1.0}Sr_{2.0}Mn_2O_7$. The M-1 transition occurs at temperatures depending on the composition of the different samples. From the ρ-T curve of the present investigation it is clear that transition temperature decreases for the higher concentration of x for the samples of the Ruddlesden-Popper family of compounds $(R_{1-x}D_x)_{n+1}Mn_nO_{3n+1}$.

Figure 4.2 show that the presence of 0 86T magnetic field in the same samples increases M-I transition temperature by few Kelvin. This would be due to the suppression of spin fluctuations with the applied field in the paramagnetic region. The external magnetic field enhances spin order that ultimately decrease the resistivity and results higher transition temperature. It is also observed that the higher percentage of Sr concentration favours insulating paramagnetic phase and lower the value of transition temperature. This is reasonable as Sr itself is an insulating material
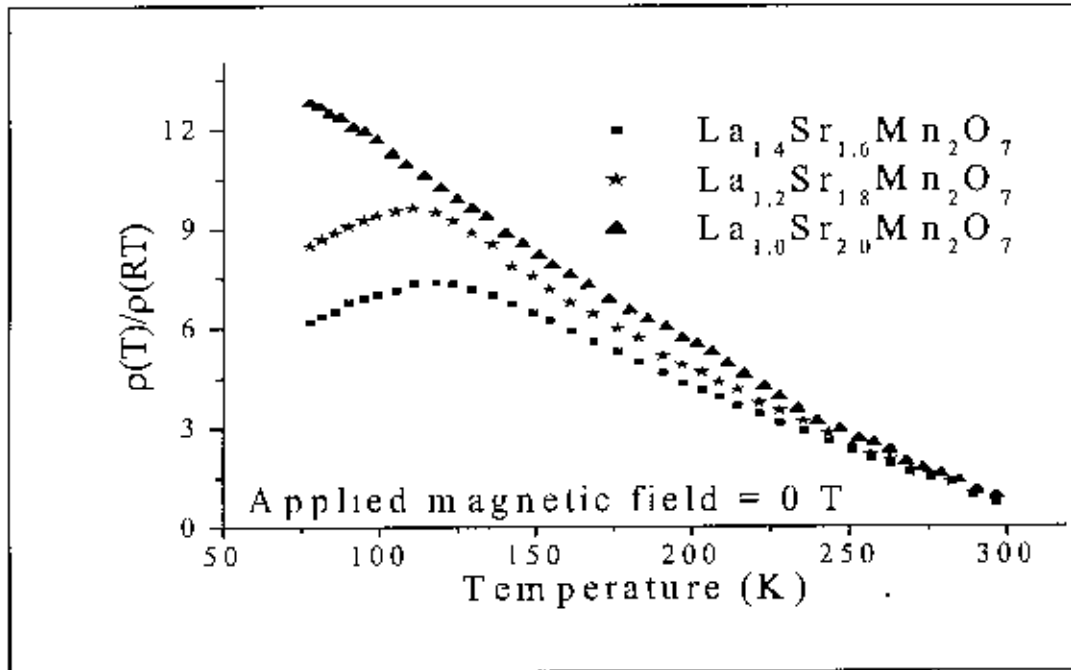
Fig.4.1: Normalized resistivity as a function of temperature for $La_{2-2x}Sr_{1+2x}Mn_2O_7$ (x =0.3-0.5) samples with the applied magnetic field 0 T
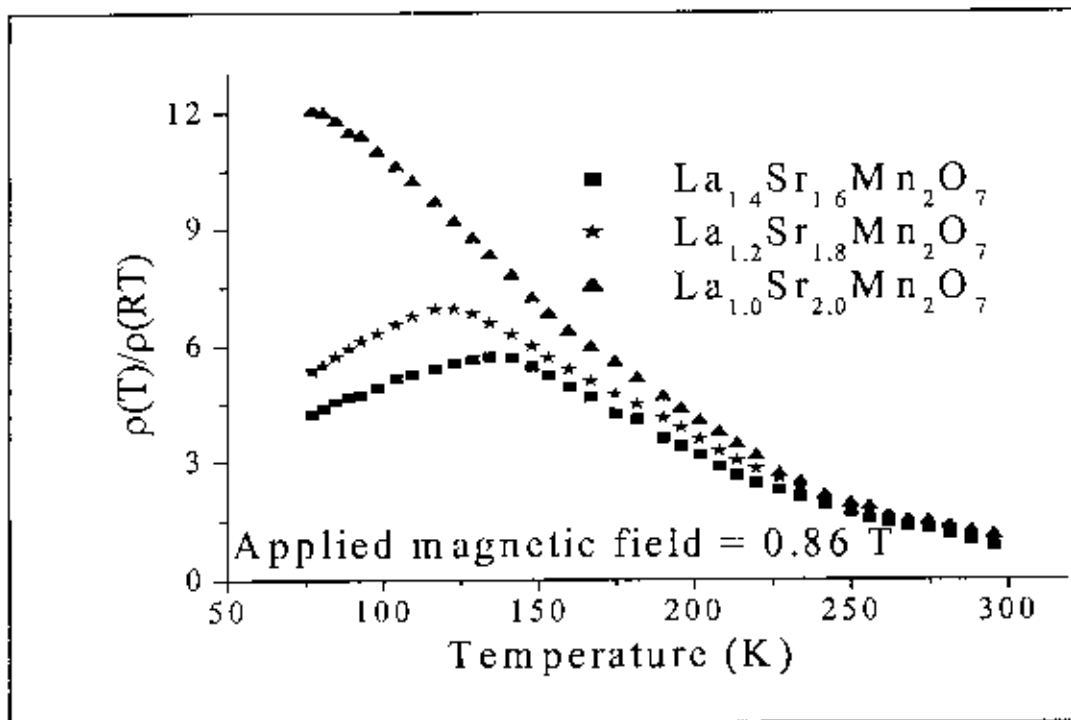
Fig 4.2: Normalized resistivity as a function of temperature for $La_{2-2x}Sr_{1+2x}Mn_2O_7$ (x =0.3-0.5) samples with the applied magnetic field 0.86 T
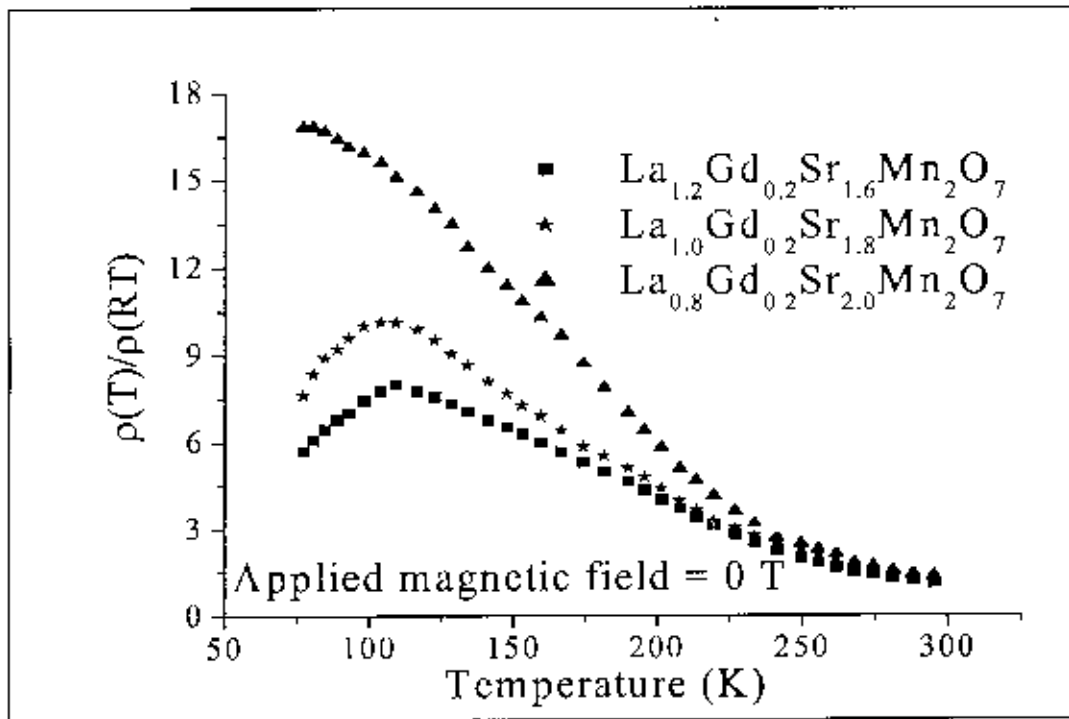
Fig 4 3: Normalized resistivity as a function of temperature for $La_{1.2}Gd_{0.2}Sr_{1.6}Mn_2O_7$, $La_{1.0}Gd_{0.2}Sr_{1.8}Mn_2O_7$ & $La_{0.8}Gd_{0.2}Sr_{2.0}Mn_2O_7$ samples with the applied mag. field 0 T
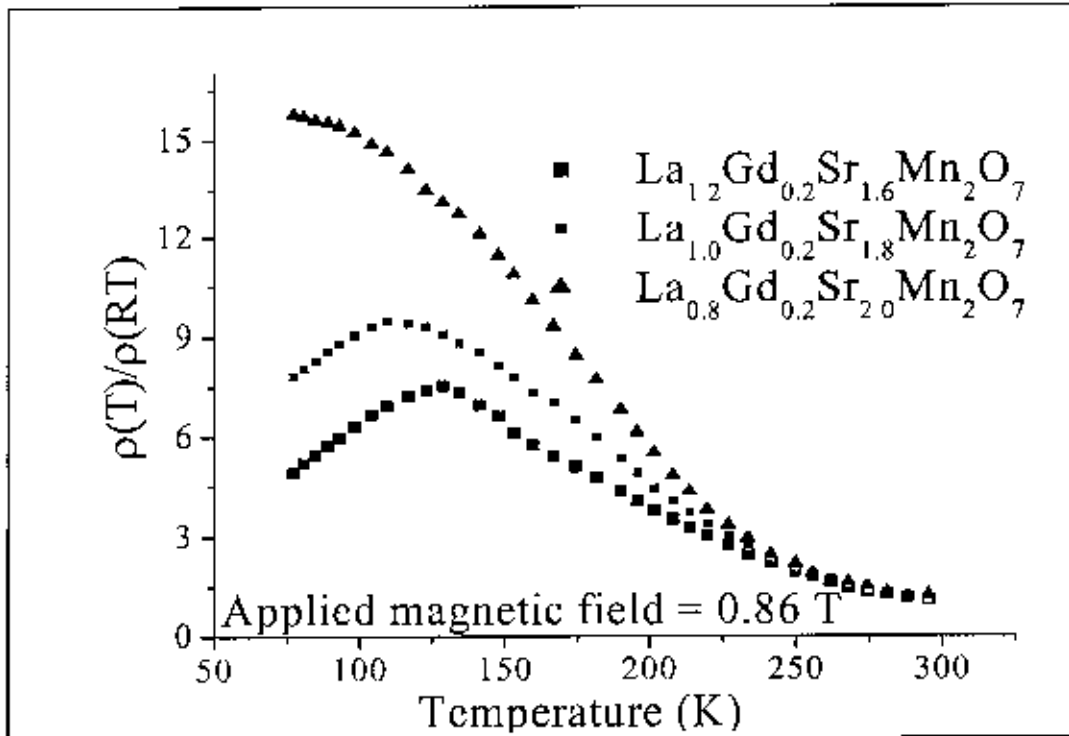
Fig. 4.4: Normalized resistivity as a function of temperature for $La_{1.2}Gd_{0.2}Sr_{1.6}Mn_2O_7$, $La_{1.0}Gd_{0.2}Sr_{1.8}Mn_2O_7$ & $La_{0.8}Gd_{0.2}Sr_{2.0}Mn_2O_7$ with the applied magnetic field 0.86 T
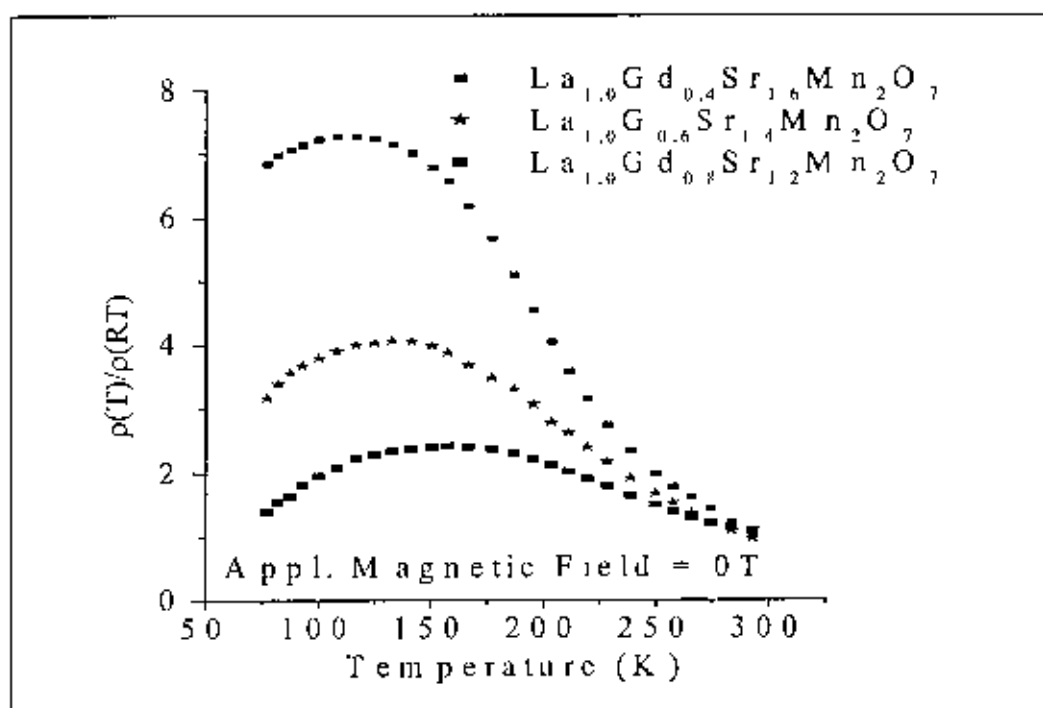
Fig 4.5. Normalized resistivity as a function of temperature for La$_{1.0}$Gd$_{0.4}$Sr$_{1.6}$Mn$_2$O$_7$, La$_{1.0}$Gd$_{0.6}$Sr$_{1.4}$Mn$_2$O$_7$ & La$_{1.0}$Gd$_{0.8}$Sr$_{1.2}$Mn$_2$O$_7$ with the applied magnetic field 0 T
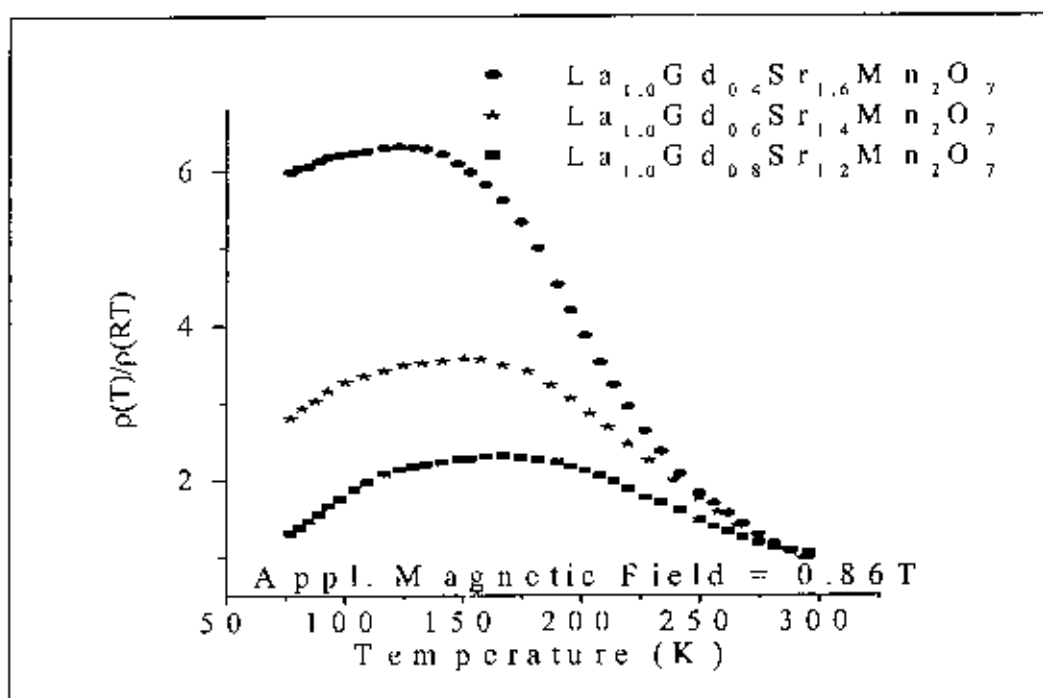
Fig 4.6: Normalized resistivity as a function of temperature for La$_{1.0}$Gd$_{0.4}$Sr$_{1.6}$Mn$_2$O$_7$, La$_{1.0}$Gd$_{0.6}$Sr$_{1.4}$Mn$_2$O$_7$ & La$_{1.0}$Gd$_{0.8}$Sr$_{1.2}$Mn$_2$O$_7$ with the applied magnetic field 0 86 T

40

Table 4.2: M-I transition temperatures Tp both at zero field and at 0.86 T applied magnetic field for various polycrystalline samples

Sample Composition	Without field (0T)		With field (0.86 T)	
	Tp (K)	$\rho(Tp)/\rho(RT)$	Tp (K)	$\rho(Tp)/\rho(RT)$
$La_{1.4}Sr_{1.6}Mn_2O_7$	117	7.37	134	5.70
$La_{1.2}Sr_{1.8}Mn_2O_7$	110	9.62	117	6.91
$La_{1.0}Sr_{2.0}Mn_2O_7$				
$La_{1.2}Gd_{0.2}Sr_{1.6}Mn_2O_7$	109	7.99	128	7.54
$La_{1.0}Gd_{0.2}Sr_{1.8}Mn_2O_7$	103	10.13	109	9.50
$La_{0.8}Gd_{0.2}Sr_{2.0}Mn_2O_7$				
$La_{1.0}Gd_{0.4}Sr_{1.6}Mn_2O_7$	116	7.27	128	6.30
$La_{1.0}Gd_{0.6}Sr_{1.4}Mn_2O_7$	141	4.40	150	3.57
$La_{1.0}Gd_{0.8}Sr_{1.2}Mn_2O_7$	152	2.45	168	2.31

Previous investigations by various researcher indicated that the M-I transition temperature is generally very close to the Curie temperature, T_c, the ferromagnetic to paramagnetic transition. Below T_c, the spin system is ferromagnetically ordered and the probability for electron transfer (and therefore the mobility) is high. Above T_c, the resistivity decreases with temperature as for an insulator, where transport is thermally activated. Near T_c, however, the spin system is highly susceptible to external field, which causes a substantial change of the local spin disorder and thereby of the carrier mobility. Thus the field drive the material more metallic. Far above the Curie point, the external field can no longer compete with the thermally induced random spin fluctuations and the resistance decreases with temperature.

In our investigation the M-I transition temperature for $La_{1.4}Sr_{1.6}Mn_2O_7$ bulk sample is observed at 118 K and 132 K at zero field and at an applied field of 0.86 T respectively. Philipp et al. [1] measured the resistivity as a function of temperature of a coherently strained $La_{1.4}Sr_{1.6}Mn_2O_7$ thin film grown on $NdGaO_3$ at different magnetic fields for the in-plane and out of plane current direction. In their investigation the resistivity

maximum associated with the FM-PI transition is observed at T_{max} ~125 K for $La_{1.4}Sr_{1.6}Mn_2O_7$ thin film. The result is very close to our present investigation of bulk $La_{1.4}Sr_{1.6}Mn_2O_7$ sample. This sort of M-I transition may be explained within the framework of interaction mechanisms between the manganese ions that occur via oxygen ions. Exchange coupling mechanism in the manganites are believed to be as follows:

(i)   Nature of the couplings are ferromagnetic when the interaction is in between Mn^{3+} and Mn^{4+} ions.

(ii)   Antiferromagnetic behavior arises for interaction between Mn^{4+} ions.

(iii) Interactions between Mn^{3+} ions can produce ferro or antiferromagnetic in natures.

In $LaMnO_3$, the valence of La (and other members of family such as Pr) is 3+, the valence of O in this composition is 2-, so the valence of Mn should be 3+ to fulfill the charge neutrality. In other words, an undoped lanthanum manganite compound corresponds to the following ionic composition $La^{3+}Mn^{3+}O_3$. The electronic configuration of neutral Mn atom is $3d^54s^2$ that means that the ionized Mn^{3+} has 4-d electrons that will be responsible for its electronic properties. If trivalent rare earth La atoms are substituted for a divalent metal such as Ca, the following compound $Ca^{2+}Mn^{4+}O_3$ with the Mn valence 4+ will be obtained. Thus, the Mn ion in the $CaMnO_3$ compound will have 3 d-electrons Both the manganites $LaMnO_3$ and $CaMnO_3$ are antiferromagnetic insulators. For a partial substitution case,

$La_{1-x}Ca_xMnO_3$ ($0<x<1$), Mn ions are mixed-valent and average number of d –electrons at the Mn site is 4-x. An amazing fact is that, although pure La and pure Ca manganites are antiferromagnetic insulators, the intermedium composition

$La_{1-x}Ca_xMnO_3$ exhibits strong magnetism (metallic conductivity and ferromagnetism) over a wide range of carrier concentrations and temperatures.

With $La_{2-2x}Sr_{1+2x}Mn_2O_7$, the fundamental mechanism leading to the appearance of metallic ferromagnetism would be the same. The parent material of $La_{2-2x}Sr_{1+2x}Mn_2O_7$ is a charge transfer insulator of $La_2SrMn_2O_7$. When divalent Sr ions are substituted in place of trivalent La to produce e.g. $La_{2-2x}Sr_{1+2x}Mn_2O_7$ charge neutrality is disturbed. To keep the material neutral a part of Mn valency changes from 3+ to 4+ in the following

42

manner $La_{2-2x}^{3+}Sr_{1+2x}^{2+}Mn_{2-x}^{3+}Mn_x^{4+}O_7^{-2}$. Thus doping the insulating $LaMn_2O_7$ material, in which only Mn^{3+} exist, with the divalent ions (Ca, Ba, Sr etc.) causes the conversion of a proportional number of Mn^{3+} to Mn^{4+}. Because of strong Hund's coupling, the electronic configurations are Mn^{3+} ($t_{2g}^3 e_g^1$) and Mn^{4+} ($t_{2g}^3 e_g^0$). The presence of Mn^{4+}, due to the doping enables the e_g electron of a Mn^{3+} ion to hop to the neighboring Mn^{4+} ion via double exchange, which mediates ferromagnetism and conduction.

Figure 4.3 and 4.4 show the normalized resistivity as a function of temperature for Gd doping on the La of $La_{2-2x}Sr_{1+2x}Mn_2O_7$ compounds at zero field and applied magnetic field of 0.86 T respectively. The substitution of Gd in place of La remaining the Sr unchanged results in lowering of metal insulator transition temperature by a few Kelvin. As Gd^{3+} is substituted for La, the valency of La and Gd remains same but the atomic sizes of La is larger than Gd ions. As a result there would be other possible interactions such as phonon mediated electron-electron interaction, electron phonon interaction, lattice distortion etc due to their different atomic sizes, crystal structure and different magnetic moments. For the different atomic sizes of the doping elements the crystal structure may distort due to Jahn -Teller effect and changes would arise in the transition peak. The double exchange, and consequently, the physical properties of these materials, is particularly susceptible to the lattice effects brought by doping. Previous experiments demonstrated that [2] very strong lattice effects have been realized when the La ions are partially replaced by trivalent and divalent ions of different sizes. That is any deviation from the ideal cubic perovskite structure can lead to either a reduction in the Mn-O-Mn bond angle from 180^0, or in the bond length, both directly affecting the double exchange. In the present investigation upon substitution of La (ionic radius ~1.22 A^0) with Gd, which has a smaller ionic radius (~1.06A^0), the MnO_6 octahedra are forced to rotate in order to compensate the resulting variation of space around A site. This rotation of MnO_6 octahedra lowers the Mn-O-Mn bond angle and thus reduces the electron hopping between Mn^{3+} and Mn^{4+} ions. Therefore, the result of replacing La by Gd atoms is found to lower the ferromagnetic (or metal-insulator) transition temperature, an effect that is due to bond bending caused by the lattice adjusting to the size differential between the La and Gd ions.

The others point of consideration is that the resistivity of FM metal has a quite pronounced contribution from the electron scattering on spin disorder (apart from the usual contribution from crystal lattice defects and electron- phonon scattering). Higher number of electrons results other types of interactions, spin fluctuations which gives rise to increase further spin disorder in the compound. As the magnetic field is applied the resistivity decreases because all the disordered spin aligns in the direction of the applied field and as a result scattering is reduced Thus the metal-insulator transition is enhanced by few kelvin as the applied magnetic field accelerates magnetic ordering. These results agree with the results reported earlier [3] for $La_{0.67}Ca_{0.33}MnO_3$ polycrystalline bulk samples and have consistency with our present investigation.

Figures 4.5 and 4.6 show the normalized resistivity behavior as a function of temperature for polycrytalline samples of the type $La_{1.0}Gd_{0.4}Sr_{1.6}Mn_2O_7$, $La_{1.0}Gd_{0.6}Sr_{1.4}Mn_2O_7$, $La_{1.0}Gd_{0.8}Sr_{1.2}Mn_2O_7$ in zero field and in an applied magnetic field of 0.86 T respectively.

To date, much of the investigation of the CMR materials have been done either by doping of the La by divalent ions or trivalent atoms of lanthanum series. In the present investigation, the Gd was substituted for Sr keeping La unchanged. From the ρ-T curve (figures 4.5 and 4.6) it is clear that when non-magnetic Sr is replaced with magnetic Gd atom the transition temperature is found to increase dramatically favoring metallic phase. The magnetic property of Gd is thought to be responsible for higher transition temperature. When Sr will be replaced by magnetic Gd, the concentration of non magnetic Sr will be reduced and the Gd-Gd coupling will increase. The ferromagnetic coupling of Gd-Gd is likely to enhance Tp, the ferromagnetic to paramagnetic phase transition temperature with increasing Gd. The reason for increasing of Tp for these samples upon the application of magnetic field is due to spin alignment and the mechanism is similar to that of the trivalent substituted samples in the La site i.e. resistivity decreases upon the application of magnetic field.

44

4.3 Magnetoresistance of various polycrystalline samples

This chapter concerns the magnetoresistive properties of the various bulk polycrystalline samples.

Typical magetoresistance curve obtained for the samples at room temperature are shown in figures 4.7 and 4.9 as a function of magnetic field. Room temperature MR is found to be very low almost 1.5% ~ 2% and is almost linear with field.

But the MR at 78 K for these polycrsytalline samples shown in Fig. 4.8 and 4.10 exhibited a large value in presence of low applied magnetic field. At low temperature (78K) the field dependence of MR exists for an applied field of upto H* as shown in figures 4.8 and 4.10. The magnetic field H* designates the boundary of the two slopes. Beyond H* the magnetoresistance is a weak function of the applied magnetic field. In this work, about 12 % ~15 % of the MR is observed at H* = 0.15 T~ 0.16 T. The maximum change in MR is 16% for $La_{1.4}Sr_{1.6}Mn_2O_7$ polycrystalline sample at H* = 164 mT whereas the total magnetoresistance for this sample is 19% under the application of 860 mT magnetic field. This may be due to the reason that as the materials are subdivided into domains, low field was quite sufficient to align the domain spins and thus a sharp decrease in MR was observed but to align the spins at the domain boundary requires much larger field leading to weak field dependence.

Previously it was observed from magnetization measurements that this H* is close to the saturation magnetization field of the sample. The two slopes MR at low temperature were explained by Hossain et al [4] in following grain and grain boundary model.

At T<<T_c the material is in the ferromagnetic regime In the absence of field the magnetization of the grain of the polycrystalline material will be like that in figure 4.11 a. The individual spins at the grain boundary regions are randomly oriented. In the absence of field, a carrier will suffer scattering from the unaligned magnetic domain, as well as disordered spin at the grain boundary region By applying a low magnetic field, the magnetization of each grain starts to align towards the direction of the external

magnetic field as shown in figure 4.11 b. However a large magnetic field is required to align the spins of the grain boundaries as shown in figure 4.11c.
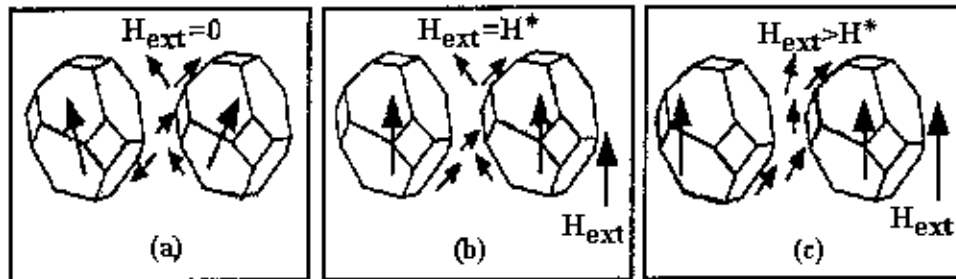

Figure 4.11: Explanation of the two sloes MR at low temperature (T <Tc)

Table 4.3: H^* at 78 K for various polycrystalline materials

Samples	Maximum H (mT)	H* (mT)	MR %	Maximum MR %
$La_{1.4}Sr_{1.6}Mn_2O_7$		164	15	19.96
$La_{1.2}Sr_{1.8}Mn_2O_7$		126	5	10 82
$La_{1.0}Sr_{2.0}Mn_2O_7$		83	2	10 81
$La_{1.2}Gd_{0.2}Sr_{1.6}Mn_2O_7$	860 mT	139	10	17.56
$La_{1.0}Gd_{0.2}Sr_{1.8}Mn_2O_7$		130	6	13.57
$La_{0.8}Gd_{0.2}Sr_{2.0}Mn_2O_7$		122	5	13.07
$La_{1.0}Gd_{0.4}Sr_{1.6}Mn_2O_7$		123	10	15.19
$La_{1.0}Gd_{0.6}Sr_{1.4}Mn_2O_7$		108	7	14.18
$La_{1.0}Gd_{0.8}Sr_{1.2}Mn_2O_7$		103	5	12.25

The magnetic properties of the grain boundary play a central role in the understanding of the magnetotransport properties in polycrystalline manganites. Hwang *et al.* [6] observed an unexpectedly large low-field magnetoresistance in polycrystalline magnetic bulk and thin film samples, which is due to the spin-polarized tunneling between ferromagnetic grains. This finding initiated numerous studies on extrinsic magnetoresistance effects in magnetic oxides; investigations were extended to other systems such as CrO, $Tl_2Mn_2O_7$ as well as to the present Ruddlesden-Popper family of compounds $(R_{1-x}D_x)_{n+1}Mn_nO_{3n+1}$. But the initial aim of fabricating magnetic field sensors operating at room temperature, however, has not yet been made. Hence the physics of spin polarized transport in both ferromagnetic tunnel junctions and grain boundary junctions has led to great challenges to both theoretical as well as experimental physics and constitutes a new research area within the emerging field of spin-electronics.
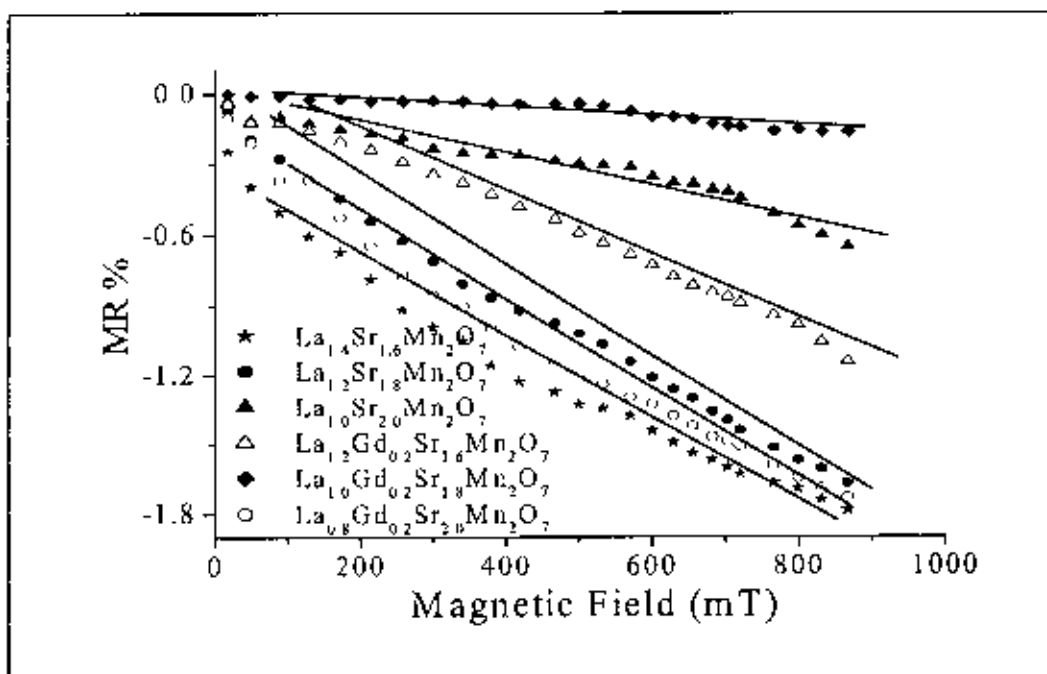
Fig. 4.7: Magnetoresistance (MR) as a function of magnetic field at room temperature for various polycrystalline samples sintered at 1100^0C
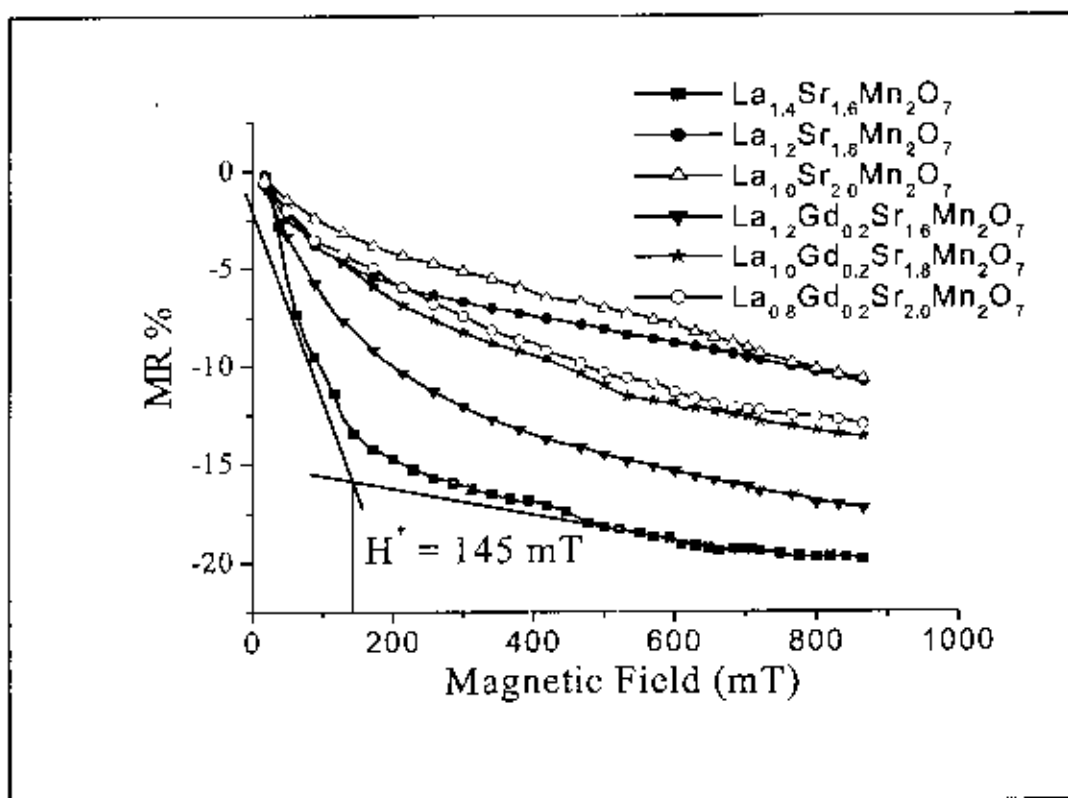

Fig. 4.8. Magnetoresistance (MR) as a function of magnetic field at 78 K for various polycrystalline samples sintered at 1100^0

48
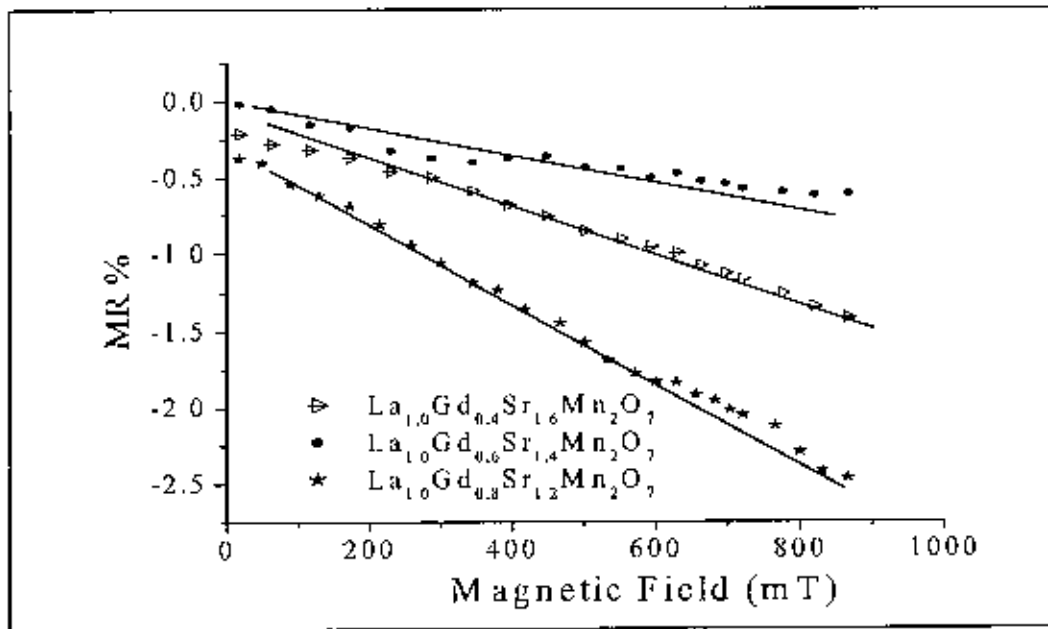
Fig 4.9. Magnetoresistance (MR) as a function of magnetic field for for $La_{1.0}Gd_{0.4}Sr_{1.6}Mn_2O_7$, $La_{1.0}Gd_{0.6}Sr_{1.4}Mn_2O_7$ & $La_{1.0}Gd_{0.8}Sr_{1.2}Mn_2O_7$ at room temperature for various polycrystalline samples sintered at 1100^0C

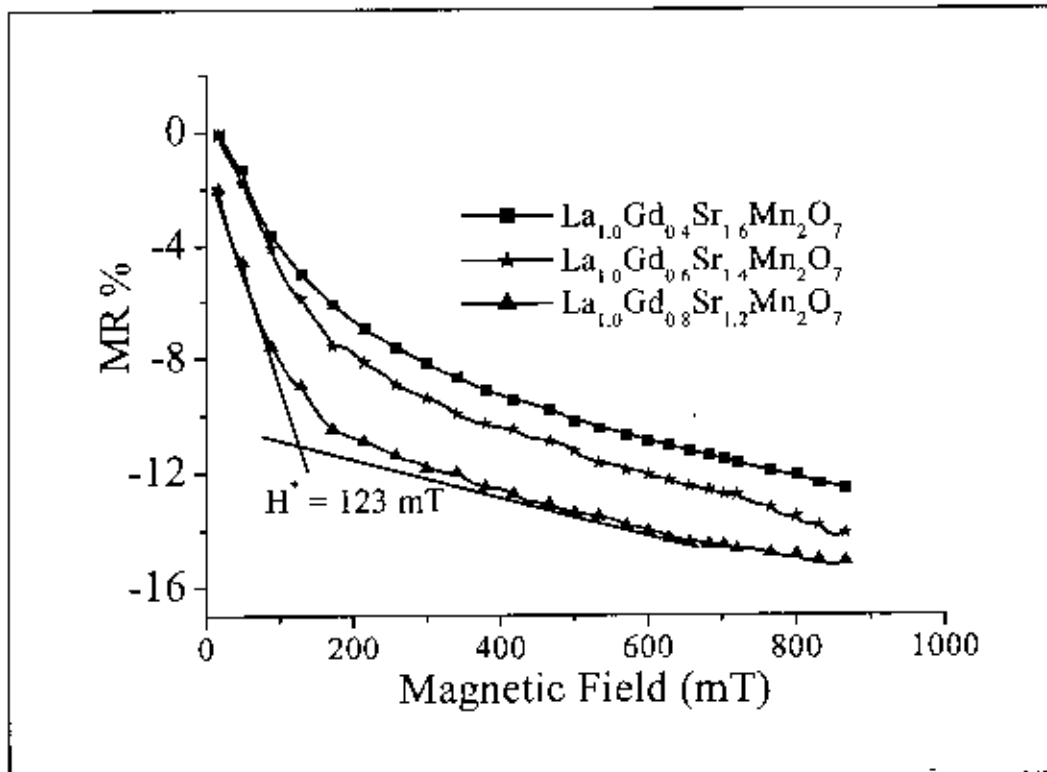Fig. 4.10 Magnetoresistance (MR) as a function of magnetic field for for $La_{1.0}Gd_{0.4}Sr_{1.6}Mn_2O_7$, $La_{1.0}Gd_{0.6}Sr_{1.4}Mn_2O_7$ & $La_{1.0}Gd_{0.8}Sr_{1.2}Mn_2O_7$ at 78 K for various polycrystalline samples sintered at 1100^0C

49

4.4. Activation Energy

Activation energies for various investigated polycrystalline samples can be calculate from the slopes of straight lines using the relation

$$\rho = \rho_0 \exp (E_0/K_B T)$$

where, E_0 is the activation energy and K_B is the Boltzmann constant

In figures 4.12 ln $\rho(T)/\rho(RT)$ is plotted against $1/T$ for various polycrystalline samples at sintering temperature 1100^0 C and applied magnetic field 0 T and 0.86 T. The temperature region is considered from transition temperature to room temperature for the respective polycrystalline samples. Table 4.4 shows the values of the activation energies.

All the samples show very good linear behavior in the ln $\rho(T)/\rho(RT) - T^1$ which suggest that conduction occurs through a thermally activated process.

Table 4.4: Activation energy (meV) of the polycrystalline samples

| Samples	Applied Magnetic Field (0T)	Applied Magnetic Field (0.86 T)
$La_{1.4}Sr_{1.6}Mn_2O_7$	24 3 ±1.31	23.9 ±1.39
$La_{1.2}Sr_{1.8}Mn_2O_7$	26.3±1.38	25 5±1 67
$La_{1.0}Sr_2 Mn_2O_7$	30 8±1.41	29 0±1 95
$La_{1.2}Gd_{0.2}Sr_{1.6}Mn_2O_7$	27.2±1.53	26.5±1.27
$La_{1.0}Gd_{0.2}Sr_{1.8}Mn_2O_7$	29.7±2.11	28.8 ±1.79
$La_{0.8}Gd_{0.2}Sr_2Mn_2O_7$	35 0±2.48	33.9 ±1.68
$La_{1.0}Gd_{0.4}Sr_{1.6}Mn_2O_7$	55.29 ±2.96	53.9 ±3.48
$La_{1.0}Gd_{0.6}Sr_{1.4}Mn_2O_7$	38.32 ±2.79	34.35 ±2.92
$La_{1.0}Gd_{0.8}Sr_{1.2}Mn_2O_7$	24.1 ±2.22	22.5 ±2.621
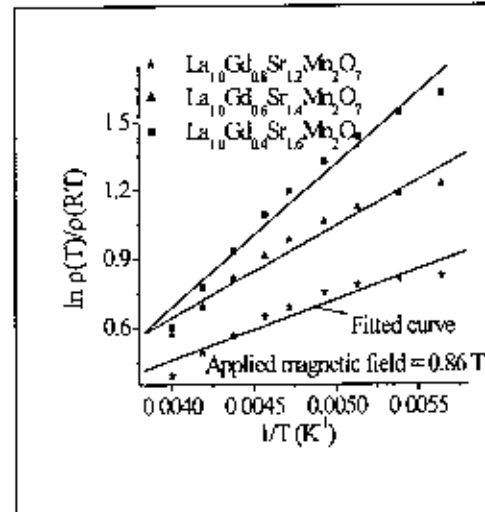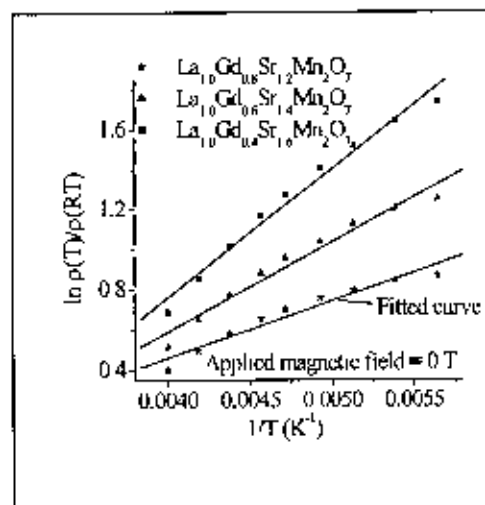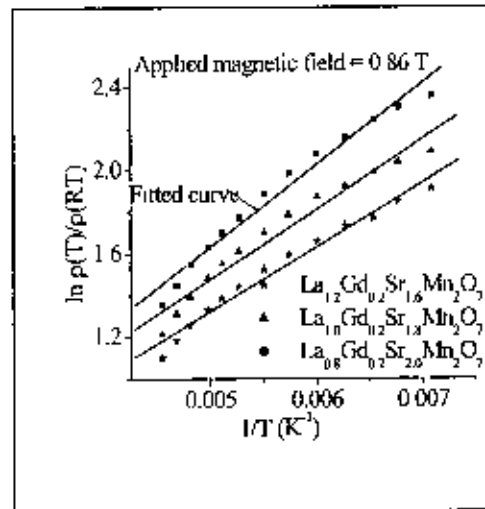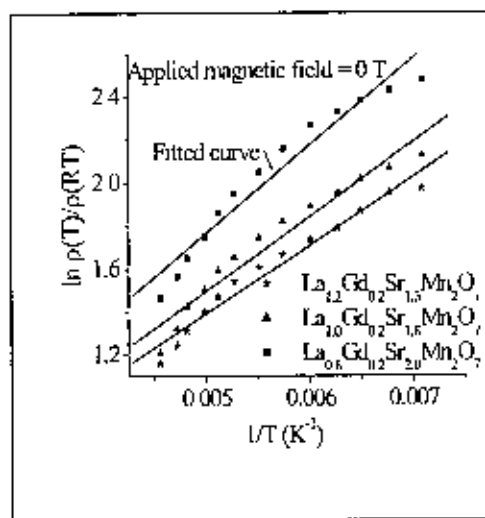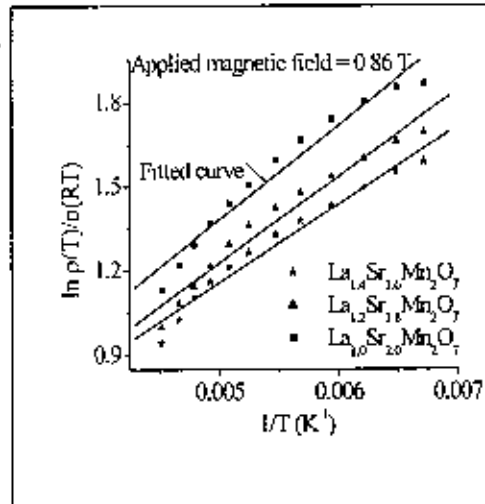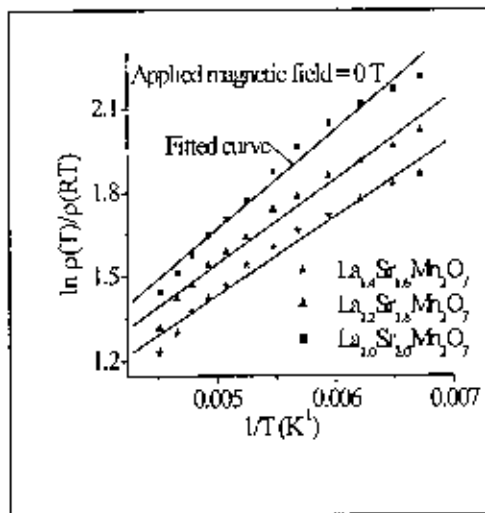
Figure 4.12: ln ρ(T)/ ρ(RT) is plotted against 1/T (K⁻¹) for various polycrystalline samples at 1100°C sintering temperature

The activation energies obtained from the slopes of the linear curves showed that it increases with the increase of concentration x in $R_{2-2x}Sr_{1+2x}Mn_2O_7$ (R = La, Gd) polycrystalline samples. It was also observed that the activation energies increases slightly with the substitution of Gd in place of La and this is due to the lower size of Gd atom. The result is in agreement with that obtained by A Barman et al [5] for $Pr_{0.7}R_{0.1}Ca_{0.2}MnO_3$ (R = Y, Dy.Gd. Sm, Nd) samples. It is also noticeable that higher percentage of Sr concentration in the samples increases activation energy.

References

[1] Philipp J B., Klein J, Recher C, Walther T, Mader W, Schmid M, Suryanarayanan L. Alff and R Gross, (2002), "Microstructure and magnetoresistance of epitaxial films of the layered perovskites $La_{2-2x}Sr_{1+2x}Mn_2O_7$ (x = 0.3 and 0.4), Phys. Rev. B, 65 184411.

[2] Ahn K.H., Wu X.W , Liu K., and Chen C.L., (1996), "Magnetic properties and colossal magnetoresistance of $La(Ca)MnO_3$ materials doped with Fe", Phys. Rev. B, 54 15 299.

[3] Akther Hossain A.K.M., Cohen L F., Dammy F., Berenov A., MacManus-Driscoll J.L., Alford N.McN., Mathur N.D., Blamire M.G. and Evetts J.E., (1999), "Influence of grain size on magnetoresistance properties of bulk $La_{0.67}Ca_{0.33}Mn_{3-\delta}$", J. Magnetism and Magnetic Materials, 192(2) 263.

[4] Akther Hossain A.K.M., Cohen L.F., Berenov A and MacManus-Driscoll J.L., 2001, "Highly sensitive low-temperature low-field colossal magnetoresistance screen printed $La_{0.63}Y_{0.07}Ca_{0.30}MnO_{3-\delta}$ Thick Films", Materials Science and Engineering, 83, 79.

[5] Barman A.. Ghosh M., Biswas S , De S. K. and Chatterjee S., (1998), " Charged ordered state and giant magnetoresistance in $Pr_{0.67}R_{0.1}Ca_{0.2}MnO_3$ (R = Y, Dy, Gd, Sm, Nd)", J. Phys : Condens. Matter 10, L199-L205.

[6] Hwang H. Y., Cheong S-W., Ong N P. and Batlogg B. (1996), "Spin-Polarized Intergrain Tunneling in $La_{2/3}Sr_{1/3}MnO_3$", Phys. Rev. Lett. 77 2041

CHAPTER 5

Summary, Conclusions and Suggestion for Further Work

Summary of the present investigation

Magnetoresistive properties of $La_{2-2x}Sr_{1+2x}Mn_2O_7$ bulk polycrystalline samples prepared for doping levels x = 0.3 -0.5 and sintered at temperature 1100^0C for 24 hours in air have been investigated from room temperature down to liquid nitrogen temperature using standard four-probe technique. X-ray diffraction (XRD) analysis was performed on these samples to examine phase purity. From the XRD pattern the samples were found to be homogeneous and single phase.

The temperature dependence of normalized resistivity of polycrystalline bulk samples $La_{2-2x}Sr_{1+2x}Mn_2O_7$ for x = 0.3 –0.5 in zero magnetic field and in a magnetic field of 0.86 T were investigated. The corresponding behavior was also observed in addition of a small amount of Gd in place of La and Sr of $La_{2-2x}Sr_{1+2x}Mn_2O_7$ bulk samples. Most of the samples show an metal-insulator transition with a peak in the electrical resistivity, ρ_P, at a temperature Tp. It is seen that with the decrease in temperature, the resistivity of the samples are increased reaching at maximum value at a certain temperature. With the further decrease in temperature the resistivity is decreased. The above-mentioned temperature is the metal- insulator transition temperature and is generally very close to the Curie temperature, Tc, the ferromagnetic to paramagnetic transition. The transition temperature varies from 103 K to 168 K with doping concentration and partial substitution of Gd on the La and Sr of $La_{2-2x}Sr_{1+2x}Mn_2O_7$ (x = 0.3 –0.5) polycrystalline samples.

It is well known that hole doping in ABO_3-type perovskite manganese oxide produces metallic conductivity and ferromagnetism where the magnetic interaction is mediated by the transfer of the holes (the double exchange interaction in the mixed Mn^{3+} /Mn^{4+} valence state). With $La_{2-2x}Sr_{1+2x}Mn_2O_7$, the fundamental mechanism leading to the appearance of metallic ferromagnetism would be the same. The parent material of $La_{2-2x}Sr_{1+2x}Mn_2O_7$ is a charge transfer insulator of $La_2SrMn_2O_7$. In hole undoped $La_2SrMn_2O_7$, the Mn^{3+} ion has the electron configuration of $t^3_{2g}e^1_g$. Among the four 3d electrons on the Mn site, t^3_{2g}electrons can be viewed as localized spins (S = 3/2), while the e^1_g electron is either

53

itinerant or localized. Substitution of La^{3+} by Sr^{2+} introduces holes into the e_g state (some Mn^{3+} ions convert into the Mn^{4+} state without e^1_g electrons).

The substitution of Gd in place of La keeping Sr unchanged results a lowering of metal insulator transition temperature. As the atomic size of Gd is smaller than that of La, the substituted Gd ions lower the Mn-Mn exchange interaction substantially by bending the Mn-O-Mn bond angle. Thus, the result of replacing La by Gd atoms is found to decrease the transition temperature, an effect that is due to bond bending caused by the lattice adjusting to the size differential between the La and Gd ions.

From the ρ-T curve it is clear that the presence of Sr enhances paramagnetic insulating phase. But when non-magnetic Sr is replaced with magnetic Gd atom the transition temperature is found to increase dramatically favoring metallic phase. The magnetic property of Gd is thought to be responsible for higher transition temperature. The replacement of Sr by magnetic Gd will increase Gd-Gd coupling and this ferromagnetic coupling of Gd-Gd is likely to enhance Tp, the ferromagnetic to paramagnetic phase transition temperature with increasing Gd.

From the observation of the ρ-T curves it is seen that the M-I transition temperature is increased in presence of the magnetic field. It may be due to the suppression of the spin fluctuations with the applied field in the paramagnetic region. The external magnetic field enhances spin order that ultimately decrease the resistivity and results higher transition temperature. It is also observed that the higher percentage of Sr concentration favours insulating paramagnetic phase and lower the value of transition temperature. This may be due to the insulating behavior of Sr.

In the present study, room temperature magnetoresistance is found to be very low almost 1.5% ~ 2% and is almost linear with field for bulk polycrystalline $R_{2-2x}Sr_{1+2x}Mn_2O_7$ (R = La, Gd) samples. Magnetoresistance measurements for the bulk samples show a sharp drop at low magnetic fields followed by a linear dependence at higher fields. The exhibited large MR effects in these compounds at low temperature and very low field might be

associated with magnetic-domain based scattering or spin-polarized tunneling between grains.

In $\rho(T)/\rho(RT) - T^{-1}$ plots for the present investigated samples suggest that conduction occurs through a thermally activated process. The activation energies obtained from the slopes of the linear curves showed that it increases with the increase of concentration x in $R_{2-2x}Sr_{1+2x}Mn_2O_7$ (R = La, Gd) polycrystalline samples. It was also observed that the activation energies increases slightly with the substitution of Gd in place of La and this is due to the lower size of Gd atom. It is also noticeable that higher percentage of Sr concentration in the samples increases activation energy.

Conclusions

Most of the samples show an insulator-metal transition with a peak in the electrical resistivity, at a temperature Tp.

The above-mentioned temperature is the metal- insulator transition temperature and is generally very close to the Curie temperature, Tc, the ferromagnetic to paramagnetic transition.

This sort of M-I transition can be explained within the framework of double exchange mechanism.

The substitution of Gd in place of La keeping the Sr unchanged results a lowering of metal insulator transition temperature.

But when non-magnetic Sr is replaced with magnetic Gd atom the transition temperature is found to increase dramatically favoring metallic phase. The magnetic property of Gd is thought to be responsible for higher transition temperature.

From the observation of the $\rho(T)$ curves it is seen that the M-I transition temperature is increased in presence of the magnetic field.

55

It is also observed that the higher percentage of Sr concentration favours insulating paramagnetic phase and lower the value of transition temperature.

In the present study, room temperature magnetoresistance is found to be very low almost 1.5% ~ 2% and is almost linear with field.

Magnetoresistance measurements for the bulk samples show a sharp drop at low magnetic fields followed by a linear dependence at higher fields.
The exhibited large MR effects in these compounds at low temperature and very low field might be associated with magnetic-domain based scattering or spin-polarized tunneling between adjacent grains.

In $\rho(T)/\rho(RT) - T^{-1}$ plots for the present investigated samples suggest that conduction occurs through a thermally activated process.

It was also observed that the activation energies increase slightly with the substitution of Gd in place of La and this is due to the lower size of Gd atom.

Suggestion for Further Work

Previous investigation by researchers indicated that metal-insulator transition
(T_{M-I}) temperature of CMR manganites is generally very close to the Curie temperature
(Tc), the ferromagnetic to paramagnetic transition. This fact should be checked for the samples of the present investigation. In spite of the enormous research effort, certain aspects of phenomena of CMR research such as spin polarized tunneling in trilayer systems, grain boundary magnetoresistance in polycrystalline manganites, domain wall scattering etc are not well understood till now. Understanding of the above mentioned phenomena is relevant for basic research as well as potential applications of magnetic oxides.

56